

**HOW THE TURTLE MAKES ITS PALATE WITHOUT
PALATAL SHELVES**

by

Kelvin Jia-Mien Leung

A THESIS SUBMITTED IN PARTIAL FULFILLMENT OF THE REQUIREMENTS FOR
THE DEGREE OF

MASTER OF SCIENCE

in

The Faculty of Graduate Studies

(Craniofacial Science)

THE UNIVERSITY OF BRITISH COLUMBIA
(VANCOUVER)

September 2011

© Kelvin Jia-Mien Leung, 2011

Abstract

Vertebrate craniofacial development and speciation has been studied in great detail, with major emphasis placed on mammalian species and highly derived archosaurs (birds). However, less is known about reptiles and in particular turtles. Turtles are speculated as to have retained many ancestral features of amniotes. Therefore, studying the Testudine (turtle) order not only helps to better understand amniote head development, but also the derivation of modern form. This thesis will investigate the formation of the hard palate in a representative turtle species, *E. subglobosa*, not only because of its evolutionary significance but also because this region is frequently affected in orofacial clefting. Origins of the palatine bones were first examined since other amniotes form these bones within outgrowths of the maxillary prominence, or the palatal shelves. Surprisingly no palatal shelves were found at the position or time when they should have been forming. Instead palatine bones condensed directly in the mesenchyme beneath the nasal cavity. Furthermore there was no evidence from cell proliferation or apoptosis analysis of the maxillary prominences that vestigial shelves were ever present. The hypothesis following was that gene expression in the maxillary prominences might be different in turtles compared to the chicken or mouse in which shelves do form. I found no major differences but interestingly several of the genes I studied were also markers of the primitive stomodeum. Results show the turtle retains gene expression patterns of the chicken stomodeum, the primitive oral roof before palatal shelf formation, suggesting the turtle oral roof is still primitive in nature rather than advanced in other amniotes. This unfamiliar mechanism of hard palate development with no vestigial traits of palatal shelf formation supports arguments for a more basal placement of the turtle in the phylogenetic tree. Contrary to these findings, the similarity in gene expression and sequence to the chicken argues for a more derived placement closer to the archosaurs. While these present results do not allow for confident placement of the turtle as more basal or derived in the amniote tree, the data collected shows that ontological studies can help shed light on evolutionary debates.

Preface

All *Emydura subglobosa* eggs were generously donated to us by the Toronto Zoo.

This research was initially reviewed by the Toronto Zoo ethics board when the collaboration was set up in 2006. The Zoo is sent a progress report each year, the contents are reviewed and approval is then renewed.

In addition the work is carried out under UBC Ethics approval # A07-0488. This protocol was originally approved Nov. 12, 2007 and has been renewed annually since then.

Table of Contents

ABSTRACT.....	ii
PREFACE.....	iii
TABLE OF CONTENTS	iv
LIST OF TABLES	vi
LIST OF FIGURES	vii
LIST OF ABBREVIATIONS	viii
ACKNOWLEDGEMENTS	ix
DEDICATION.....	x
CHAPTER 1 - INTRODUCTION.....	1
1.1 AMNIOTE PHYLOGENY	1
1.2 PHYLOGENY OF THE ORDER TESTUDINES.....	6
1.3 THE TURTLE SKULL	7
1.4 NEURAL CREST ORIGINS OF THE SKULL	9
1.5 FORMATION OF FACIAL PROMINENCES, FUSION OF THE PRIMARY PALATE.....	10
1.6 MOLECULAR SIGNALING IN THE FACIAL PROMINENCES.....	11
1.7 OBJECTIVES OF RESEARCH	14
CHAPTER 2 - MATERIALS AND METHODS	15
2.1 SPECIMEN COLLECTION	15
2.2 WHOLEMOUNT SKELETAL ANALYSIS	15
2.3 HISTOLOGICAL SECTIONS	15
2.4 CELL PROLIFERATION	16
2.5 CELL APOPTOSIS.....	17
2.6 SECTION IN-SITU – RADIOACTIVE DETECTION.	17
2.7 CLONING OF TURTLE CDNAs.....	17
2.7.1 Degenerate primer design.....	17
2.7.2 Degenerate PCR.....	18
2.7.3 TA Cloning of PCR products	18
2.8 PHYLOGENETIC ANALYSIS TOOLS:	19
CHAPTER 3 - RESULTS	21
3.1 PALATE DEVELOPMENT IN EMYDURA, SEQUENCE OF OSSIFICATION AND HISTOLOGY	21
3.1.1 Wholemound staining and micro CT analysis shows that the hard palate is comprised of the palatine processes of the maxillary bones, palatine, pterygoid and vomer bones 21	
3.1.2 There are no palatal shelves in Emydura subglobosa.....	25
3.2 CELLULAR DYNAMICS.....	28
3.2.1 Apoptosis is not increased on the medial side of the maxillary prominence	28

3.2.2	<i>Cell proliferation is not decreased on the medial side of the maxillary prominence.</i>	29
3.3	GENE EXPRESSION IN THE EMBRYONIC TURTLE FACE	33
3.3.1	<i>Expression of Bmps during palate morphogenesis</i>	33
3.3.2	<i>Expression of Shh and Fgf pathway genes</i>	38
3.3.3	<i>Transcription factors downstream of the Fgf, Hh and BMP signaling pathways are expressed in the turtle palate</i>	41
3.4	MOLECULAR PHYLOGENY OF EMYDURA SUBGLOBOSA GENES	44
3.4.1	<i>Bmp phylogenetic analysis</i>	47
3.4.2	<i>Fgfr phylogenetic analysis</i>	47
3.4.3	<i>PTCH phylogenetic analysis</i>	48
CHAPTER 4 - DISCUSSION		49
4.1	PALATAL SHELVES ARE ALWAYS A PRECURSOR TO HARD PALATE FORMATION IN MAMMALS.....	49
4.2	POSTERIOR CHOANAE TISSUE MAY LANDMARK A HOTSPOT FOR CELL SIGNALING IN E. SUBGLOBOSA.	50
4.3	THE MECHANISM OF PALATE FORMATION OF E. SUBGLOBOSA MAY BE SIMILAR TO CROCODILIANS.	51
4.4	USING PALATE ONTOGENY TO PLACE TURTLES IN THE PHYLOGENETIC TREE.....	53
4.5	USING MOLECULAR PHYLOGENY AS A TOOL FOR PHYLOGENETIC DISCRIMINATION OF TURTLES.....	54
4.6	CONCLUSIONS	57
REFERENCES.....		59

List of Tables

Table 3.1 DNA sequences of <i>E. subglobosa</i> cloned fragments.	35
Table 3.2. Accession Numbers of Phylogenetic Tree Sequences.....	46
Table 4.1. Arguments for the evolutionary placement of the turtle derived from data in this thesis.	58

List of Figures

Figure 1.1 Amniote phylogeny, evolution of the palate	4
Figure 1.2 The earliest fossil of a turtle, Proganochelys, from Gaffney, 1979.....	5
Figure 2.1 - PhyLIP bootstrapping and distance algorithm parameters.....	19
Figure 2.2 - PhyLIP parameters regarding neighbour-joining protein distance phylogenetic trees.	20
Figure 3.1 – Wholemout skeletal staining and Micro CT of <i>E. subglobosa</i> skulls	24
Figure 3.2 – Histology of the developing primary and secondary palate in <i>E.subglobosa</i>	27
Figure 3.3 Cellular dynamics in the developing <i>E. subglobosa</i> palate	31
Figure 3.4 – BrdU data in graphical format.....	32
Figure 3.5 – <i>Bmp2</i> and <i>Bmp4</i> Gene expression of <i>E. subglobosa</i> stage 3 and 4.	36
Figure 3.6 – <i>Bmp7</i> and <i>Ptch1</i> Gene Expression of <i>E. subglobosa</i> stage 3 and 4.	37
Figure 3.7 – <i>Fgf</i> pathway genes <i>Fgfr2</i> and <i>Spry2</i> in <i>E. subglobosa</i> stage 3 and 4.....	40
Figure 3.8 - <i>Msx2</i> and <i>Twist1</i> Gene Expression in <i>E. subglobosa</i> stage 3 and 4	43
Figure 3.9 – <i>Bmp</i> , <i>Fgfr2</i> , and <i>Ptch1</i> protein phylogeny and orthology	45
Figure 4.1. An overview of palatal shelf formation through amniote evolution.	56

List of Abbreviations

as - alisphenoid
b - brain
Bmp - bone morphogenetic protein
bo - basioccipital
BrdU - Bromodeoxyuridine
bs - basisphenoid
c - choanae
cDNA - complementary DNA
d - dentary bone
DNA - deoxyribonucleic acid
e - eye
et - egg tooth
Fgf - fibroblast growth factor
fnp - frontonasal prominence
ios - interorbital septum
j - jugal bone
lnp - lateral nasal prominence
mc - Meckel's cartilage
md - mandibular bone
Msx - msh homeobox
mxh - maxillary bone
nb - nasal bone
nc - nasal capsule
np - nasal pit
ns - nasal septum
o - otic vesicle
oc - optic chiasma
p - palatine bone
pa - parietal bone
pf - prefrontal bone
pm - premaxilla
po - post-orbital bone
pt - pterygoid bone
Ptch - patched
RNA - ribonucleic acid
RT-PCR - reverse transcriptase polymerase chain reaction
Shh - sonic hedgehog
sq - squamosal bone
st - stomodeum
tc - trabeculae cranii
TUNEL - Terminal deoxynucleotidyl transferase dUTP nick end labeling
vno - vomernasal organ

Acknowledgements

I offer my gratitude to the faculty, staff, and my fellow students in the faculty dentistry at the University of British Columbia. The support and service of those within the department has inspired my past work and future endeavours.

I thank Dr. Joy Richman for accepting me into her laboratory and guiding me throughout the past three years. Her role in my academic and personal growth was essential in the completion of my program. I could not have asked for a better mentor to spur me towards better things.

I thank the Natural Sciences and Engineering Research Council of Canada, who funded this project as a grant to Dr. Richman.

I am indebted to Andrew Lentini of the Toronto Zoo for expertly collecting, packing up and sending me the turtle embryos.

I thank those I have come to befriend during my term in the Richman laboratory. My utmost thanks to Kathy Fu. The radioactive experiments would not have been a possibility without your expertise and efficiency. Along with assisting with the apoptotic data, answering plethora of questions, and picking up after me (both the times I've noticed and the times I haven't), you have contributed to a major part of this project.

I extend my thanks to Gregory Handrigan, who taught me the experimental procedures when I first entered the laboratory and mentored my first steps into the graduate program. His encouragement, support, and friendship will always be remembered.

I thank Sara Hosseini for her diligent work during the long in-situ days, and for all the talks and smiles in and out of the laboratory. Thank you Suresh and Poongodi, Nori, and Cheryl Whiting.

I am thankful to Dr. Ravindah Shah for the talks and conversations on evolutionary biology and scientific research as a whole, as well as his support in my academic growth.

I thank Churmy Fan for her endearing friendship during the past three years. The days at the laboratory would have gone by twice as slow without your banter and personality.

Special thanks are owed to my parents, who have supported me throughout my many years of education. Even during my hardest days, their constancy in love and encouragement allowed me to weather life's storms with a heart of peace.

Dedicated to my parents Aden and Leah Leung

CHAPTER 1 - INTRODUCTION

1.1 *Amniote phylogeny*

This thesis will be studying a species of turtle called *Emydura subglobosa*. In order to provide some evolutionary context to the work, the position of turtles within the vertebrate phylogenetic tree will first be reviewed. Evolution of vertebrate animals over the millennia has led to the formation of 2 major lineages: the agnathans which have no jaws (eg. lamprey and hagfish) and the gnathostomes, which have jaws. The gnathostomes evolved further to the osteichthyes (bony fish), chondrichthyes (sharks), amphibians, and at the crown of the tree are the amniotes (Carroll, 1988; Pough et al., 2005). It is within the amniotes that turtles are located.

Modern amniotes are a group of tetrapod vertebrates (four-footed animals with backbones or spinal columns) that have a terrestrially adapted life form. Thus amniotes comprise most of the vertebrates living on land in our modern world. Amniotes are aptly coined since the amniote embryo develops inside an egg which contains extra embryonic membranes (amnion, chorion and allantois). Within the amniote group there was a very early split into two lineages, the synapsids (mammals) and the sauropsids (avian and non-avian reptiles, Fig. 1.1). Since reptiles share a common ancestor with mammals and branched off at the same time as mammals they are not more primitive than mammals. During the Permian period, Sauropsids branched further into two lineages: the Archosaurs and Lepidosauromorphs. Archosaurs include all extant and extinct crocodiles, dinosaurs, and birds. Lepidosauromorphs include living lizards, sphenodon, snakes and their respective extinct relatives (Carroll, 1988). Birds are the most recent radiation of amniotes with fossils dating back to the Jurassic period. In contrast to birds, turtles appear much earlier, during the Upper Triassic period. The fossil that supports the emergence of turtles during this period is *Proganochelys* (Fig. 1.2; (Gaffney, 1979) and is presumed to be the ancestor from which all other turtles may have evolved. This fossil was easily recognizable as belonging to the order of Testudines because of its shell (carapace). However the mystery is that before the first turtle, no intermediate animals displayed had rudimentary shells. Then suddenly in the Upper Triassic period, turtles appear in the fossil record. This has driven paleontologists to speculate that there has been either a rapid evolution of the shell or a restricted environment in which conditions did not favour fossilization of biological materials.

While there has never been any disagreement regarding placing turtles in the Sauropsid taxon, there still is no agreement on their position relative to other reptiles. Turtles may be rooted as sister to either the lepidosauria, archosauria (Hedges and Poling, 1999), or even basal to both groups (Carroll, 1988; Rieppel, 1999; Werneburg and Sanchez-Villagra, 2009). Historically, turtles were placed basal to Lepidosauria and Archosauria, and thus closer to the stem amniote based on their skull morphology. Turtles have no temporal openings (anapsids) whereas mammals are synapsids (one opening) and other reptiles are diapsids (two openings; Fig. 1.1. Paleontologists have classically hypothesized the stem amniote to exhibit the anapsid condition like the turtle. Extinct turtles had the same anapsid skull morphology as extant turtles and so far there are no fossils that disprove these findings. However, there are two mechanisms in which this morphology could have arisen. Either the basal condition for all reptiles, or it could be a derived condition which is an adaptation from the diapsid reptilian skull. is clearly supported (Werneburg and Sanchez-Villagra, 2009).

Some paleontologists believe turtles are phylogenetically ancient based on their skull, carapace, and limb morphology (Shaffer et al., 1997). In addition, a developmental biologist has taken the basal side of the argument (Werneburg and Sanchez-Villagra, 2009). These authors looked at external characteristics of turtle embryos and compared these to birds, the sphenodon, echidna, opossum, armadillo, lizard, alligator. Due to timing of morphogenesis, these authors place the turtles in a basal position relative to the living saurian clades. The molecular phylogenists however paint a different picture.

The introduction of DNA sequencing technology in the late eighties and early nineties not only accelerated the fields of genetics and experimental medicine, but also evolutionary biology. For the first time, scientists were able to categorize species of animals according to an unbiased data set. With the new methods, researchers did not have to depend entirely on comparisons of morphology which was the traditional way of defining a monophyletic clade. With the advent of molecular sequencing, turtle placement within the phylogenetic amniote tree the past two decades has been tumultuous. During the mid-nineties Rieppel and deBraga scrapped the traditional view of placing turtles as basal to diapsids and argued for a sister group relation to lepidosaurs (squamates and tuatara) based on morphological and molecular attributes (Rieppel and deBraga, 1996; deBraga and Rieppel, 1997). However, sequencing nuclear DNA alone yielded a grouping of turtles with the crocodiles (Hedges and Poling, 1999). Different

methods of phylogenetic data interpretation also changed evolutionary turtle placement. Parsimony algorithms clashed against maximum likelihood models and gave very differing interpretations to same data sets (Zardoya and Meyer, 2001).

However, as more and more researchers tackle this question of phylogenetic placement of the turtle by analysing mitochondrial and nuclear DNA of turtles, the most consistent result is that turtles are a sister group to birds and dinosaurs (Shaffer et al., 1997; Zardoya and Meyer, 1998; Hedges and Poling, 1999; Cao et al., 2000; Zardoya and Meyer, 2001; Sasaki et al., 2004; Iwabe et al., 2005; Krenz et al., 2005; Jungt et al., 2006; Le et al., 2006; Parham et al., 2006; Shedlock et al., 2007; Naro-Maciel et al., 2008; Russell and Beckenbach, 2008; Zhang et al., 2008; Burke, 2009; Spinks and Shaffer, 2009; Spinks et al., 2009; Valenzuela, 2009; Janes et al., 2010). In a complementary approach, karyotyping showed high linkage conservation between birds and turtles (*P. sinensis*) (Matsuda et al., 2005).

These more recent molecular results are surprising since birds possess highly derived characters such as feathers and wings. Moreover, the dating of the first appearance of birds puts them after the first dinosaurs appeared on Earth (Zhou, 2004). Turtles and birds diverged from their common ancestor more than 210 MYA (Matsuda et al., 2005). The argument of turtles being a sister group to aves on the evolutionary tree of life is contrary to a more basal position supported by fossil records (Gaffney, 1979; Carroll, 1988), comparative morphology of embryo characters (Werneburg and Sanchez-Villagra, 2009) and the adult post-orbital skull (Sheil, 2003; Sheil, 2005; Tulenko and Sheil, 2007). This discrepancy between morphological and molecular data has always been difficult to resolve and other approaches may prove useful.

Figure 1.1 Amniote phylogeny, evolution of the palate

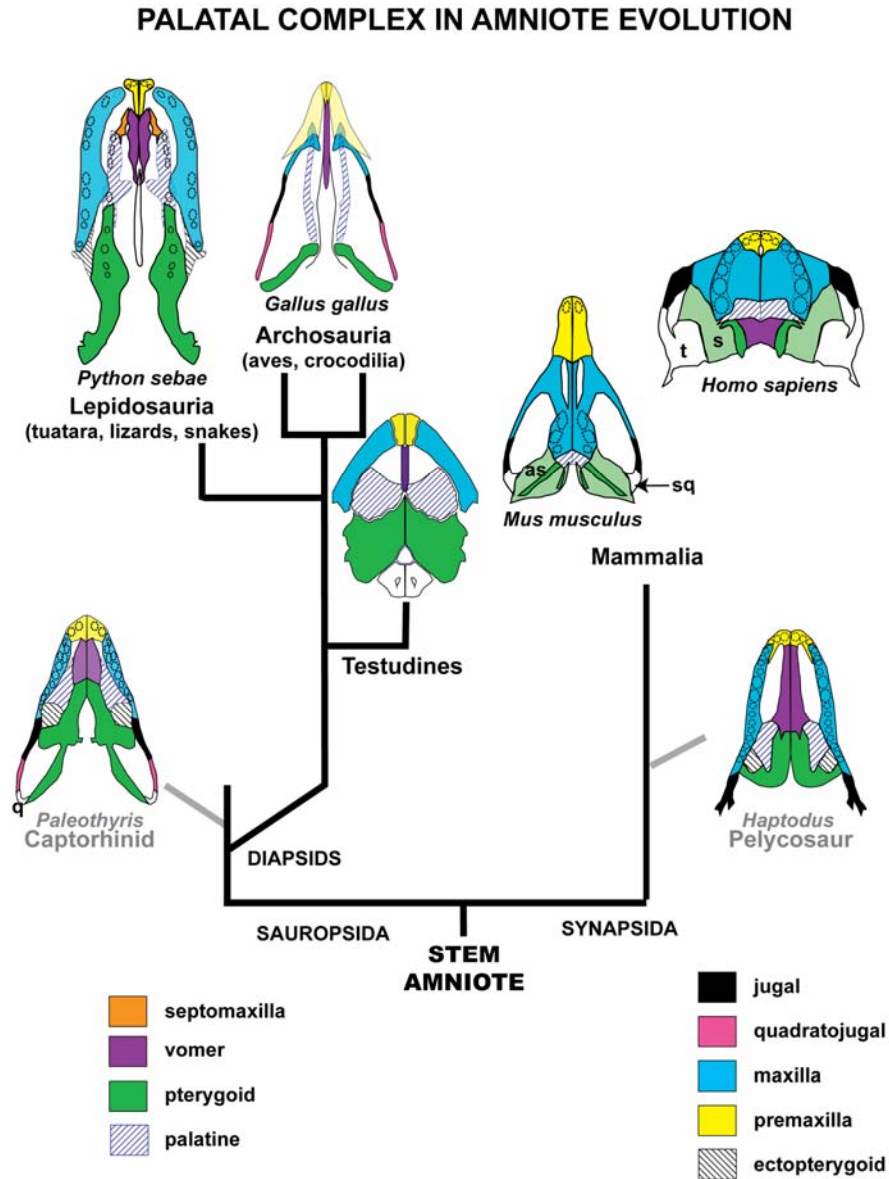


Figure 1.1. Amniote phylogeny, evolution of the palate. A sketch representation of various palates of representative amniotes. In this tree, the representative of Testudines is *Emydura subglobosa*, and is shown as being more derived and closer to the Archosaurs. This is different from the conventional placement of Testudines at a more basal location before the diapsid condition was established within the Sauropsida category. Captorhinid and Pelycosaur are extinct whereas other animals depicted are extant. Key: as – alisphenoid, sq, squamosal bone. Modified from Richman et al., 2006.

Figure 1.2 The earliest fossil of a turtle, *Proganochelys*, from Gaffney, 1979

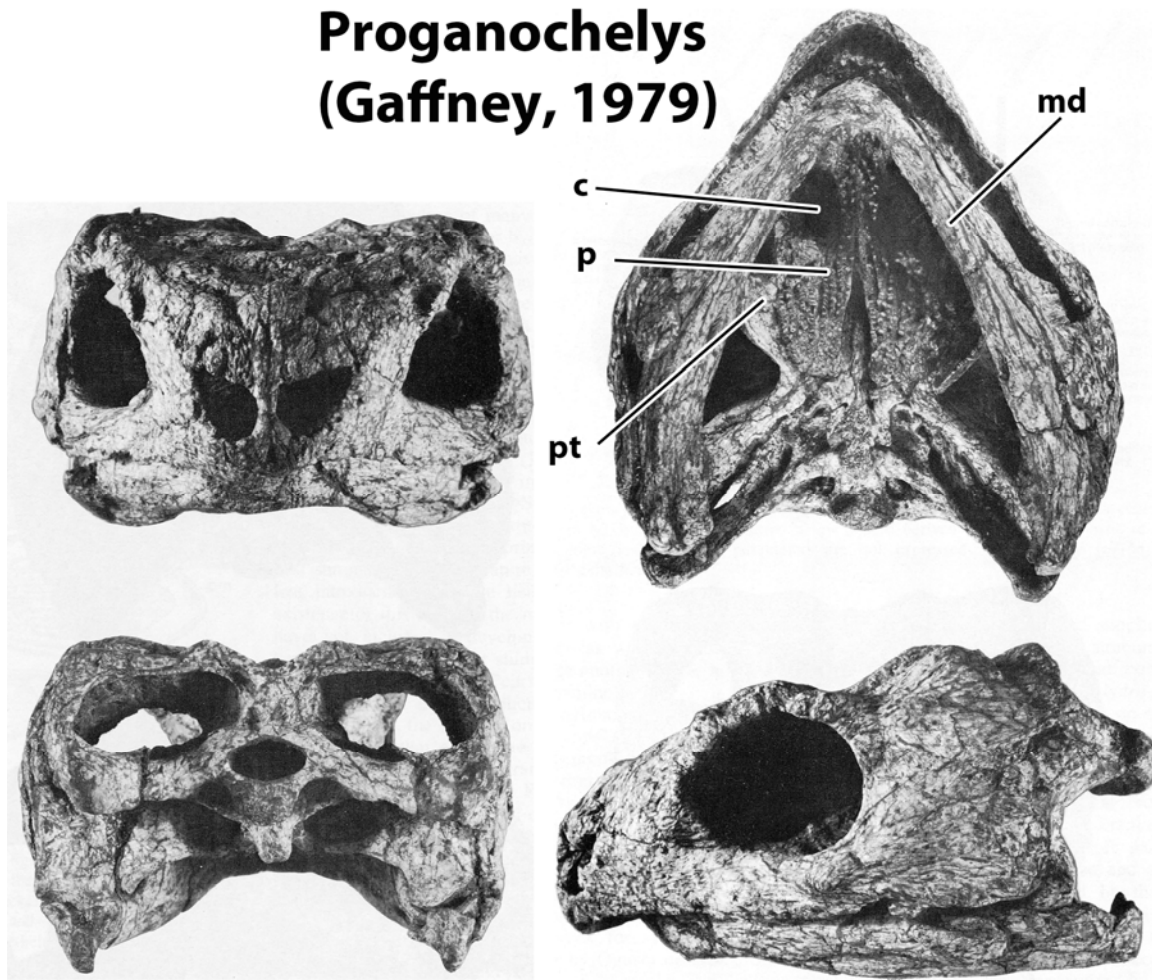


Figure 1.2. *Proganochelys*, the earliest fossil of a turtle. Characteristic bones of the palate are identifiable even in such an ancient species. The palatine bones are just anterior of the pterygoid bones in the same vertical plane, with large anterior nares (choanae) anterior to the palatine bones. Key: md, mandibular bone; c, choanae; p, palatine bone; pt, pterygoid. This figure is take directly from Gaffney, 1979.

1.2 *Phylogeny of the order Testudines*

There are two suborders of modern or extant turtles: the Cryptodira and the Pleurodira. The naming of these suborders is based upon the method of head retraction within each group. Cryptodira display specialized cervical vertebrae allowing them to retract their head into their shell along the vertebral axis. Pleurodira do not exhibit such specialized articulation, and instead fold their neck to the side. Fossil records show the suborder of Cryptodira to appear in the Upper Jurassic period, while Pleurodires do not appear until the Lower Cretaceous.

Despite their earlier appearance in the fossil record, the Cryptodira are considered to be the more advanced group of turtles. According to Gaffney (Gaffney, 1984) the Cryptodiran line is composed of two subdivisions. The extinct subdivision Pleurosternoidea is comprised of the family Pleurosternidae (Glyptopsidae, Jurassic). The subdivision Daiocryptodira, includes Baenoidea (family Baenidae, Cretaceous-Eocene), and Eucryptodira, which includes living cryptodirans (Gaffney, 1984). Cryptodires are much more diverse as compared to the Pleurodire suborder. Modern cryptodires may be grouped into three superfamilies: the Testudinoidea (tortoises and freshwater turtles), the Chelonioidea (sea turtles) with flipper limbs and reduced shell, and the Trionychoidea (soft-shelled turtles). Gaffney has postulated the *Chelonioidea* and *Trionychoidea* as monophyletic, while the *Testuinoidea* as potentially representing a more primitive aspect of cryptodire evolution and a potential base pattern from which *Chelonioidea* and *Trionychoidea* evolved.

Emydura subglobosa is a member of the suborder Pleurodira. Pleurodira are considered by the majority of experts to be more primitive than the Cryptodira although they appear 50 million years later in the fossil record than the Cryptodirans. The earliest known Pleurodiran fossils are *Notoemys laticentralis* and *Platycheilus oberndorfi* from the Late Jurassic (Gaffney, 1975b). The Pleurodira suborder consists of the two living families, Pelomedusidae and Chelidae, as well as the extinct family Araripemydidae.. The Pelomedusidae group has only three extant genera: Pelomedusa, Pelusios (Africa and Madagascar), and Podocnemis (Madagascar and South America). *Emydura subglobosa* is one of the Chelids which are represented by seven extant genera, located in South America, Australia, and New Guinea. All living pleurodires reside in fresh water niches.

A comparison of external features of Cryptodire and Pleurodire embryos has been carried out (Werneburg and Sanchez-Villagra, 2009) There are some interesting differences in the rate of

development of the mandibular process. In the Pleurodira order (*E. subglobosa*) the out growth of the mandibular process is accelerated when compared to a Cryptodire embryo of the equivalent stage. One hypothesis postulates earlier jaw musculature development as necessary for the fast prey capture methods of the Pleurodire group (Werneburg et al., 2009)

My project examines development of *E. subglobosa* which is native to Australia and Papua New Guinea. Taxonomic synonyms include *Emydura albertisii* {Boulenger, 1888 #254} and *Euchelymys subglobosa*. {Krefft, 1876 #255}. Common names are the Jardine River Turtle, Red-bellied Short-necked Turtle, and Red-bellied Shortneck Turtle. While endangered as a species in Australia, *E. subglobosa* is abundant in Papua New Guinea and is used for local consumption and trade as pets. *E. subglobosa* is a terrestrial freshwater turtle and is commonly seen in shallow and murky areas of water.

1.3 The turtle skull

The typical reptilian skull is distinguishable from mammals by several key features: in the upper jaw there are prominent pterygoid and vomer bones and the jaw joint consists of the quadrate bone which lies between the skull and mandible (diphasic). There are also several reptilian bones that are not present in mammals such as the ectopterygoid and septomaxillary bones (Boughner et al., 2007). These features are shared with the earliest amniotes in the fossil record (the Family Captorhinidae, reptilian like mammals, Fig. 1.1). Turtles have some reptilian skeletal elements but have lost the supratemporal and lacrimal bones during the course of evolution. Cryptodires have retained the epipterygoid bone, while Pleurodires have also lost this particular bone.

The temporal region of the turtle skull is flattened compared to the bird or squamate reptiles. Instead of a jugal bar that juts outward from the head, the jugal is generally a part of the orbital wall and articulates with the post-orbital bone (Gaffney, 1979). The jugal bar is only present in the diapsid reptiles and it is the lack of this structure that leads to the classification of turtles as anapsids.

The turtle hard palate is very different from squamate reptiles in that it is a contiguous set of bone that spans the roof of the oral cavity. In birds, snakes and lizards there is a naturally occurring midline gap (Fig. 1.1). The skeletal elements contributing to the turtle palate are the palatine processes of the maxilla, vomer, palatine and pterygoid bones. Thus the midline is

comprised of the vomer, palatine and pterygoid bones rather than being a single suture as in mammals. In the turtle as with many reptiles (except crocodilians), the palatine process of the maxillary bones are reduced. In the anterior region of the turtle hard palate the vomer extends up to reach the premaxillary bone. However rather than the premaxilla making direct contact with the maxillary bone as in mammals or the palatine bone as in birds, there are bilateral openings between the nasal and oral cavity, the internal nares or choanae. The choanae are located at the boundary of the primary and secondary palate. This communication between oral and nasal cavities is why the turtle cannot be classified as having a complete secondary palate. Instead it is termed an incomplete palate.

The Cryptodira and Pleurodira suborders can be distinguished on the basis of their palate anatomy. Pleurodira lack the articulation between the vomer and prefrontal bone seen in all Cryptodira. Consideration to not generalize too widely from *E. subglobosa* is important in this study since variation in skeletal anatomy within suborders have been reported. For example, in a subfamily of Pleurodira, the Pelusidid group, the vomer is absent. Nonetheless the majority of drawings in Gaffney (1979) of living turtles from either group (Cryptodira or Pleurodira) show similar palatal anatomy to *E. subglobosa*.

The sequence of ossification of the cranial bones of *E. subglobosa* has been described. Generally bones of the dermatocranium (jaws) form first, then those of the splanchnocranium (skull base) and lastly those of the neurocranium (skull vault). The first bones observed to be stained for ossification were the dentary and maxilla in the dermatocranium (Werneburg et al., 2009). This timing coincides with the onset of Alizarin stain staining of the axial elements, and has been classified as specimen or stage 5 (Werneburg et al., 2009). After 3.5 days of incubation, 'specimen 6' showed that the majority of the dermatocranial elements have ossified. These include the angular, frontal, jugal, palatine, parietal, postorbital, premaxilla, prefrontal, pterygoid, surangular, and squamosal bones (Werneburg et al., 2009). 'Specimen 7' showed nasale ossification, but vomer ossification interestingly did not occur till 'specimen 9'. Ossification of the splanchnocranial quadrate and neurocranial elements such as the basisphenoid and supraoccipital were not apparent until 'specimen 11' (Werneburg et al., 2009). Therefore quite good macroscopic skeletal differentiation data of *E. subglobosa* is available, but to date there are no histological studies describing the earlier stages during organogenesis.

1.4 Neural crest origins of the skull

The inquiry into craniofacial development of the turtle embryo includes the study of embryonic facial mesenchyme. Since this mesenchyme originates from neural crest cells, it is important to review the origins and contributions of neural crest cells to the head.

Neural crest populations originate from the dorsal folds of the neural tube along the entire length of the embryo. The origins of facial neural crest cells are from the primitive forebrain (prosencephalon), midbrain (mesencephalon) and anterior hindbrain (rhombencephalon) (Creuzet, 2005). DiI injections into the neural tube provided the first view of live, migrating neural crest cells (Lumsden et al., 1991). The fluorescently tagged cells migrated in three distinct streams. Facial crest formed one large sheet separated by a crest free region at rhombomere 3, the second group originated from rhombomere 3 and the most caudal group from rhombomeres 6 and 7. Due to the gap at r3, facial neural crest cells do not mix with those that go into the neck.

The contributions of the neural crest cells to the differentiated tissues of the head have been mapped accurately using transplants of quail neural crest cells into chicken. These methods were discovered by Nicole LeDouarin (Le Douarin, 1969) and continue to be used up to the present day to identify quail cells in the host chicken embryo at the histological level (Le Lievre, 1978; Noden, 1978; Noden, 1983; Couly et al., 1993). Neural crest cells are multipotent progenitor cells and give rise to a variety of cell types including: peripheral nervous system sensory neurons, glia, smooth muscle cells in blood vessels, melanocytes, subsets of endocrine and paraendocrine cells, and most importantly for this study, the ectomesenchyme of the head, which will give rise to cartilages and intramembranous bones. This is a unique attribute of head ectomesenchyme, as the rest of the vertebrate body's trunk neural crest is unable to derive intramembranous bones. (Couly et al., 1993; Kontges, 1996; Abzhanov et al., 2003).

Once facial neural crest cells have moved ventrally, they form the mesenchyme of the face. This is often called ectomesenchyme because it once was neural ectoderm that transformed into mesenchyme (Creuzet, 2005). The mesenchyme congregates in the facial prominences which form a ring around the primitive oral cavity or stomodeum. Neural crest cells from the prosencephalon migrate into the frontal nasal process, into the optic capsule and beneath the diencephalon where they form the roof of the oral cavity (Le Lievre, 1978; Noden, 1978). The lateral nasal prominence is populated by a combination of prosencephalic and mesencephalic

neural crest. Mesencephalic neural crest cells also contribute to the maxillary processes and mandibular arch.

In general, all cartilages and bones of the facial and oral regions (including the frontal, prefrontal, nasal, maxilla, premaxilla, parasphenoid, palatine, pterygoid, squamosal bones, and lower jaw skeletal elements) are of neural crest origin (Noden, 1978). Particular bones stemming from the prosencephalic origin include the nasal bones, the vomer, the most anterior part of the maxillaries and palatines as well as the premaxillaries. Mesectodermal cells stemming from the first branchial arch form the mandibular bones.

1.5 Formation of facial prominences, fusion of the primary palate

The vertebrate face develops from 4 pairs of facial prominences, the medial nasal (called the frontonasal mass in reptiles), the lateral nasal, maxillary and mandibular prominences. The frontonasal mass and lateral nasal prominences flank the margins of the invaginating nasal placode. The maxillary prominences originate partially from the first pharyngeal arch and partially from post-optic mesenchyme. The frontonasal mass, lateral nasal and maxillary prominences fuse to form the upper lip and anterior region of the upper jaw. The mandibular prominences are located on the inferior border of the oral cavity and ultimately form the entire lower jaw.

After the primary palate has fused, palatal shelves begin to develop on the medial sides of the maxillary prominences. These shelves in avian and squamate reptiles grow out above the tongue but fail to meet in the midline (Shah and Crawford, 1980; Shah et al., 1987; Shah et al., 1988; Buchtova et al., 2007).

Mammalian secondary palate formation differs from that of reptiles. The palatal shelves are initially vertically positioned on either side of the tongue and then reorient horizontally. Fusion occurs when the bilayered medial edge epithelium is removed and a mesenchymal bridge forms (Gritli-Linde, 2007). The fusion leads to a complete separation of the oral and nasal cavities, creating an advanced or complete secondary palate. This morphology is characteristic of extant and extinct mammals (Carroll, 1988). When a defect in fusion occurs in humans the resulting cleft interferes with function to such an extent that surgical repair is needed.

The palatal shelves in mammals give rise to the palatine processes of the maxillary bones as well as the entirety of the palatine bones. These bones support the hard palate and form a

midline suture. In addition, the palatine processes of the maxillary bone form a suture with the premaxillary bone. As a result, there are no openings between the oral and nasal cavity in the hard palate unlike in the turtle. In other reptiles such as birds and squamates, the palatine process of the maxillary bone and palatine bones are also formed within the palatal shelves. However as mentioned previously, since the shelves do not make contact, there remains a persistent cleft. We hypothesize that although there are differences in the contribution of bones to the turtle hard palate compared to other amniotes, at a minimum, the palatine bones will originate within palatal shelves.

1.6 Molecular signaling in the facial prominences

The growth and development of the head requires precise spatio-temporal signaling interactions between molecules, cells, and tissues. Such a complex system requires intricate and stringent control over developmental processes in order for components to come together and form the skull. In particular, major developmental pathways Sonic hedgehog (SHH), fibroblast growth factors (FGFs), and bone morphogenetic proteins (BMPs) are essential in growth and differentiation of the head.

In the frontonasal mass the early stages of outgrowth are controlled by the caudal edge epithelium. Removal of this small strip of epithelium prevents outgrowth of the mesenchyme (Hu et al., 2003). The boundary between the oral and extraoral epithelium has been called the frontonasal epithelial zone (Hu et al., 2003). Gene expression studies in chicken embryos have shown the stomodeal side of the epithelium expresses *SHH* whereas the external surface expresses *FGF8* (Hu et al., 2003). Initially *FGF8* is expressed across the entire frontonasal mass epithelium but then is restricted to the caudal edge. This zone of epithelium has been proposed to determine mammalian versus avian face shape (Hu and Marcucio, 2009b).

Mutually inhibitory interactions were discovered between *FGF8* and *SHH* whereby SHH is required but not sufficient to restrict *FGF8* expression dorsally, and FGF8 beads are sufficient but not required to restrict *SHH* expression ventrally (Hu et al., 2003). Instead of single molecules being able to orchestrate all of frontonasal patterning, it is the combined actions of both *SHH* and *FGF8* that are required (Hu et al., 2003; Hu and Marcucio, 2009a; Hu and Marcucio, 2009b). Additional functions of FGF signaling are to regulate proliferation of the frontonasal mass mesenchyme (Szabo-Rogers et al., 2008). Here the source of *FGF8* is not the

FEZ but is the nasal slit epithelium. Thus other epithelia surrounding the frontonasal mass in addition to the FEZ influence morphogenesis of the frontonasal mass.

In the maxillary prominence there is also a boundary zone between intraoral *SHH* expression and extraoral *FGF8* expression. In this prominence *FGF8* is localized to the maxillo-mandibular cleft and *SHH* is primarily on the medial surface of the maxillary prominence marking the position where future palatal shelves will grow out.

The corners of the frontonasal mass or globular processes and the medial edges of the maxillary prominences participate in lip fusion thus it is critical that they grow out sufficiently. Work from our lab has shown that there is surprising low proliferation in the globular processes and that instead of adding cells on at the tips, the most growth occurs in proximal mesenchyme (Szabo-Rogers et al., 2008). A similar pattern is observed in the maxillary prominence. The globular processes are under the regulation of BMPs rather than FGFs. Antagonizing FGFs specifically in the globular process has no effect on morphogenesis (Szabo-Rogers et al., 2008) whereas blocking or increasing BMP signaling prevents fusion of the lip (Ashique et al., 2002a).

There are at least three BMPs expressed in the frontonasal mass and maxillary prominences. *BMP4* transcripts are mainly found in the epithelium covering the globular processes, frontonasal epithelial zone and anterior maxillary prominence epithelium (Francis-West et al., 1994; Ashique et al., 2002a). *BMP2* is expressed highly in the globular process mesenchyme as well as the overlying epithelium as well as the medial mesenchyme of the maxillary prominence (Francis-West et al., 1994; Ashique et al., 2002a). In general, mesenchymal *BMP2* expression is stronger in than for *BMP4* (Ashique et al., 2002a). *BMP7* is strongly expressed in all epithelial surfaces and also in the caudal mesenchyme of the frontonasal mass (Lee et al., 2001; Ashique et al., 2002a; Foppiano et al., 2007). *BMP7* overlaps *SHH* in the roof of the stomodeum (Lee et al., 2001; Foppiano et al., 2007). The role of BMPs and in particular *BMP4* in determining the thickness of the upper beak has been shown in comparative studies on Darwin's Galapagos finches where increased levels of *BMP* expression correlate with thicker beaks (Abzhanov et al., 2004; Mallarino et al., 2011). In addition manipulating the level of *BMP* signaling in the frontonasal mass or maxillary prominence dramatically alters the size of the chicken beak (Ashique et al., 2002b; Wu et al., 2004; Wu et al., 2006; Foppiano et al., 2007; Hu et al., 2008). In addition implanting BMP soaked beads into the maxillary prominence of chickens leads to a duplication of the palatine bone (Barlow and Francis-West, 1997). Thus BMP

signaling is a key regulator of the intramembranous bones and cartilages comprising the facial skeleton.

There is a great deal of cross talk between the FGF, SHH and BMP pathways. Our lab and others have shown that BMPs have a negative influence on the expression of FGF8 and vice versa (Ashique et al., 2002a). BMPs influence *SHH* expression as well as shown by the increase in *SHH* expression in the presence of Noggin soaked beads (Ashique et al., 2002a). A Noggin retrovirus does not induce *SHH* but instead reduces expression (Foppiano et al., 2007). This may be an indirect effect of the virus acting via the mesenchyme which then affects epithelial *SHH* expression.

One possibility that might explain the cross talk is that fact that several of these pathways share common downstream transcription factors. BMP proteins are able to increase *MSX1* and 2 expression in the face (Barlow and Francis-West, 1997; Lee et al., 2001; Ashique et al., 2002a; Higashihori et al., 2010). Similarly FGFs are able to strongly induce *MSX* genes (Szabo-Rogers et al., 2008; Higashihori et al., 2010). SHH has a unique set of downstream mediators, Gli transcription factors and it is not known whether they can regulate expression of FGFs or BMPs.

Although we can easily observe the functional specificity of each gene in craniofacial development, it is the amalgamation of all these functions that allows the head to develop normally. Slight variations in such signaling pathways as *SHH*, *BMP*, and *FGF* pathways and their downstream targets have already been shown to alter facial growth and morphology. Thus I will focus on these three pathways in the turtle. I will begin by carrying out comparative gene expression studies. Differences in gene expression may help direct hypotheses as to why the turtle skull differs in morphology.

1.7 *Objectives of research*

The first goal of this project's research is to better understand amniote palate development through studying a rarely studied member of this group, the turtle. While extinct and extant adult turtle skulls have been explored by others in the past, very few studies have been carried out on embryos. There is a void of information on predifferentiation stages of development which will specifically be addressed in this study. A combination of approaches including histology, analysis of cell dynamics, *in situ* hybridization and whole skull staining will be utilized. This will potentially provide evidence of conserved developmental mechanisms leading to formation of the hard palate.

The second goal is to use the data to position the turtle in the amniote tree of life. By analyzing early morphology, cellular dynamics and gene expression of the maxillary prominences and primitive stomodeum, insight into evolutionary relationships of turtles to other reptiles will be gained.

CHAPTER 2 - MATERIALS AND METHODS

2.1 Specimen collection

Emydura subglobosa specimens were received from the Toronto Zoo by overnight Fedex shipment. Eggs were buried in vermiculite during travel as well as incubation at UBC. Vermiculite containers kept warm with heat packs during travel. Temperature and humidity of shipment recorded by electronic reader from the Toronto Zoo. Upon receiving shipment, eggs were wiped with double distilled water with iodine tincture to limit fungal growth. Eggs were stored at either room temperature or at 30 degrees Celsius, and hydrated every two days with normal tap water.

Turtle eggs were windowed at regions away from the embryo to minimize tissue damage. By shining incandescent light through the shell of the turtle egg (candling), I was able to locate the approximate location of the embryo. Appropriate stage for sacrifice was determined by candling and observing size of embryo and development of amniotic blood vessels. When ready for sacrifice, eggs were brought out of the 30 degree room and acclimatized to room temperature.

2.2 Wholemound skeletal analysis

Embryos used for skeletal analysis were washed in 1x PBS and transferred into 100% ethanol for 4 days. Specimens were then changed into 100% acetone for another 4 days, and stained with Alcian blue and alizarin red for 10 days as described (Boughner et al., 2007). Embryos were then cleared with 2% potassium hydroxide in 20% glycerol then changed into 50% glycerol. For micro-CT specimens were fixed in 100% ethanol and scanned in a Scanco scanner (lab of T.M. Underhill).

2.3 Histological sections

Sections on slides for histology were dewaxed in xylene (2x 20 minutes) and then hydrated through ethanol series to 100% double-distilled water. Slides were then dyed with Picrosirius red and Alcian blue for bone and cartilage staining respectively (Buchtova et al., 2007). Slides were then dehydrated back into 100% ethanol, washed in xylene, and coverslipped with Shandon EZ-mount.

2.4 Cell proliferation

BrdU labeling in vivo: A hole was cut into the shell as close as possible to the embryo using candling to locate its position. Using a 1mL syringe with a 26 gauge 3/8 bevel needle, I injected 10uL of 10mM BrdU into the yolk of the egg. Eggs were then wrapped in a Kim wipe moistened with double-distilled water, placed into vermiculite, and incubated for three hours at 30 degrees Celsius to allow for BrdU incorporation. Embryos were extracted from the egg with dissecting scissors and forceps, washed in 1X cold PBS, and then transferred into 4% paraformaldehyde for fixing overnight at 4 degrees Celsius. Quick fixing is essential at this stage to preserve RNA integrity essential for in-situ experiments. Embryos were then stepped into 70% ethanol with PBS washes (twice), 50% ethanol, and then finally stored in 70% ethanol. Specimens older than stage six (Werneburg et al., 2009) were administered 10uL of MS222 anesthetics and left for 20 minutes before extraction from egg. These specimens were then demineralized in a solution of 12.5% EDTA/4% paraformaldehyde at 4°C. Length of demineralization time depended on stage of embryo but could be as long as 2 months.

Cell proliferation was studied using a bromodeoxyuridine (BrdU) assay. BrdU is a synthetic nucleoside that is a thymidine analogue. When administered to the living embryo, cells in S phase incorporate the synthetic nucleoside into replicating DNA. Incorporated BrdU is then detected by fluorescent antibodies that recognize unique epitopes of the synthetic nucleoside. Antigen retrieval was carried out using 10 mM sodium citrate buffer, pH 6.0 for 30 min in a steamer. I also used a further pretreatment which consisted of incubating the sections in Sau3AI enzyme (NEB buffer #1) at a final concentration of 15U/ml to unmask the DNA in cells. I used a kit (GE Healthcare) in which the mouse monoclonal antibody to BrdU is also mixed with nucleases. The monoclonal antibody was applied overnight at 4° in a humidified chamber. Secondary antibodies were applied (1:200, rabbit anti-mouse conjugated to Alexa 488 (Invitrogen) and slides coverslipped with Prolong Gold containing DAPI (Invitrogen)(Handrigan et al., 2010; Handrigan and Richman, 2010).

To quantify the proportion of proliferating cells, sections were photographed at 16X magnification and stitched together using Adobe Photoshop. A grid was placed on top which divided the maxillary prominence into 6^{ths}. Cell counts in the blue (DAPI, nuclei) and green (Alexa 488, BrdU labeled cells) channels were made using the Image J plug-in, cell counter. A total of 7 stage 3 specimens and 4, stage 4 specimens were analyzed. A single section from each

embryo was analyzed thus there were no technical replicates. The right and left sides of each embryo were counted and considered as biological replicates, thus there were 14 biological replicates for stage 3 and 7 for stage 4 (the left maxillary prominence was torn in one of the stage 4 specimens). The data for the 6 regions at each stage was analyzed using 1 way ANOVA and significant differences between groups determined using Tukey's post-hoc test (Statistica, v 6.0).

2.5 *Cell apoptosis*

Apoptosis studies utilized Terminal transferase dUTP nick end labeling (TUNEL). The Apo-tag kit from Chemicon (S7111) was used for the TdT reaction at 0.3U/uL, and labeling was carried out using the FITC-dUTP analog from Roche Diagnostics. FITC anti-dig antibody was applied to the slides as per the directions in the kit. Slides were then post-fixed with 4% paraformaldehyde and mounted in Prolong Gold.

2.6 *Section in-situ – radioactive detection.*

Radioactive in-situ followed procedures as explained by Rowe et. al. 1992 (Rowe et al., 1992). Photographs of gene expression were taken with bright and darkfield illumination using a Leica M125 stereo microscope.

2.7 *Cloning of turtle cDNAs*

cDNA was transcribed from stage 1 and 3 total embryos. At this early stage, we expect the majority of signaling and transcription factors to be transcribed in abundance. Embryos were snap-frozen in liquid nitrogen and then processed through Qiagen's RNeasy Midi kit for Isolation of Total RNA from Animal Tissues. cDNA was created from this RNA stock with Invitrogen's Superscript III Reverse Transcriptase and an oligo-dT primer or random primers using the cDNA archive kit from ABI.

2.7.1 *Degenerate primer design*

Gallus gene sequences orthologous to E. subglobosa genes of interest were found on the NCBI GenBank database utilizing the 'Gene' search option (<http://www.ncbi.nlm.nih.gov/>). This protein sequence was then BLASTed against the protein database (<http://www.ncbi.nlm.nih.gov/blast/Blast.cgi>) to compile a list of orthologous genes from other species. A wide variety of taxa were selected for primer creation, with specific emphasis on

including avian, amphibian, mammalian and reptile species. Protein sequences in FASTA format were run through Blocksmaker to generate the blocks format output needed for CODEHOP analysis of primer selection. CODEHOP output produced potential primer sequences. Favourable sequences chosen had low degeneracy scores (less than 16), decent in amplicon length (600-900 base pairs), with forward and reverse primer pairs being close in annealing temperatures.

2.7.2 Degenerate PCR

The primary challenge of amplifying specific cDNA fragments by degenerate RT-PCR is to determine the optimal reaction conditions. The optimal temperature for each primer pair was decided through gradient PCR with annealing temperatures ranging from 50-55°C. Platinum Taq (Invitrogen) which is the proof-reading form was used for this first amplification step. Cycling conditions included a 3-min initial denaturation step, 35 cycles, and a 10-min final extension step. PCR reactions were run on a 1% agarose gel, and then DNA fragment band of the predicted size was extracted from with the Qiaquick Gel Extraction kit (Qiagen). After extraction and purification of DNA from agarose medium, a second-round of PCR was carried out, using the gel purified product. This repetition gives a product with greater enrichment for the target amplicon. This second PCR reaction was carried out using Taq polymerase (non-proof reading so that Ts are added to the ends of the amplicon permitting subsequent T-A cloning).

2.7.3 TA cloning of PCR products

PCR amplicons of predicted sizes were isolated from gel medium, and cloned into pGem-T Easy Vector System kit (Promega) according to the manufacturer's protocol. After overnight incubation at 4°C this ligation mix was then transformed into DH5 α competent bacteria for replication. Ampicillin-treated plates were treated with 40uL each of X-Gal (40mg/mL) and IPTG (0.1M) before bacterial plating in order to screen for colonies with inserts.

After overnight incubation, bacterial colonies positive for insert were then used to inoculate 5mL cultures which were grown overnight at 37°C. Plasmid was purified using a standard alkaline-lysis DNA mini-prep protocol, and concentrations were read by Nano-drop spectrometry. Samples with robust concentration and nucleotide purity were then sent to

Genewiz (New Jersey) for sequencing. Sequence results from Genewiz were BLASTed against the protein database using Blastx to confirm sequence identity.

2.8 *Phylogenetic analysis tools*

FASTA format amino acid sequences were input into Clustal to create a multiple alignment of an appropriate file format for use in PhyLIP 3.16, the phylogenetic construction software used in this study. Phylip Software was downloaded from www.evolution.genetics.washington.edu/phylip.html and installed on a local PC computer.

As a first step, the Clustal alignment (PHYLIP formatting) was fed into SeqBoot.exe to create 100 sample replicates of the aligned data set.

The seqboot file was then input into protdist.exe programs to create distance matrices.

Figure 2.1 - PhyLIP bootstrapping and distance algorithm parameters

```

Bootstrapping algorithm, version 3.69
Settings for this run:
D   Sequence, Morph, Rest., Gene Freqs?   Molecular sequences
J   Bootstrap, Jackknife, Permute, Rewrite? Bootstrap
%   Regular or altered sampling fraction?   regular
B   Block size for block-bootstrapping?    1 (regular bootstrap)
R   How many replicates?                   100
W   Read weights of characters?            No
C   Read categories of sites?             No
S   Write out data sets or just weights?   Data sets
I   Input sequences interleaved?          Yes
0   Terminal type (IBM PC, ANSI, none)?   IBM PC
1   Print out the data at start of run     No
2   Print indications of progress of run  Yes

Y to accept these or type the letter for one to change

Protein distance algorithm, version 3.69
Settings for this run:
P   Use JTT, PMB, PAM, Kimura, categories model? Jones-Taylor-Thornton matrix
G   Gamma distribution of rates among positions? No
C   One category of substitution rates?       Yes
W   Use weights for positions?               No
M   Analyze multiple data sets?             Yes, 100 data sets
I   Input sequences interleaved?            Yes
0   Terminal type (IBM PC, ANSI)?           IBM PC
1   Print out the data at start of run       No
2   Print indications of progress of run     Yes

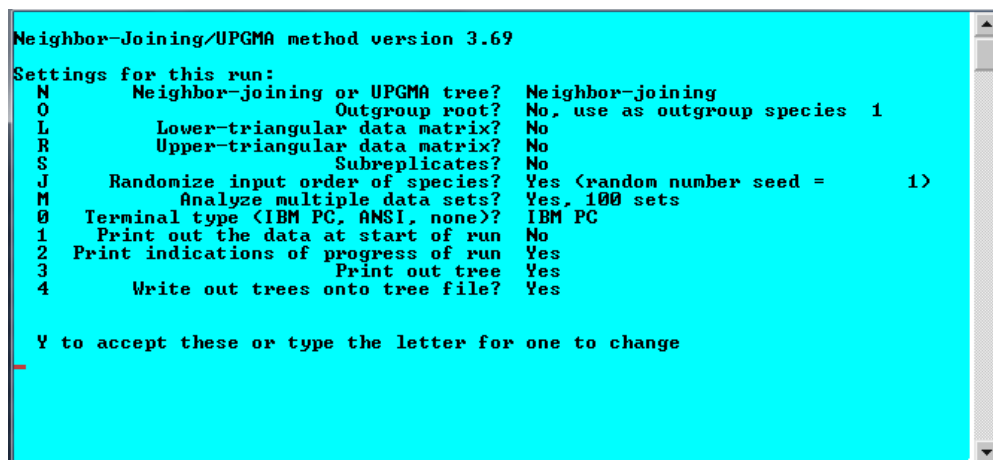
Are these settings correct? (type Y or the letter for one to change)

```

Protdist.exe output files were then analyzed by NeighbourJoining.exe. This program can generate distance trees by either the UPGMA or Neighbor-Joining method.

NJ.exe next generates 100 different trees based on 100 different bootstraps. Running the neighbor-joining output tree file through Consense.exe gives the best summary or average of the set of 100 trees. Final consensus product gives a tree with bootstrap values and optimum branching according to distance methods.

Figure 2.2 - PhyLIP parameters regarding neighbour-joining protein distance phylogenetic trees



```
Neighbor-Joining/UPGMA method version 3.69
Settings for this run:
N      Neighbor-joining or UPGMA tree?  Neighbor-joining
O      Outgroup root?                  No, use as outgroup species 1
L      Lower-triangular data matrix?    No
R      Upper-triangular data matrix?    No
S      Subreplicates?                   No
J      Randomize input order of species? Yes (random number seed = 1)
M      Analyze multiple data sets?      Yes, 100 sets
0      Terminal type (IBM PC, ANSI, none)? IBM PC
1      Print out the data at start of run No
2      Print indications of progress of run Yes
3      Print out tree                    Yes
4      Write out trees onto tree file?   Yes

Y to accept these or type the letter for one to change
```

Consensus output tree files may be viewed with TreeView 1.6.6 and displayed as different styles and outgroup parameters.

CHAPTER 3 - RESULTS

3.1 *Palate development in Emydura, sequence of ossification and histology*

The formation of the secondary palate is interesting because this is a region of the skull that has a high degree of variation amongst amniotes (Richman et al., 2006). By analyzing the secondary palate of the turtle a better understanding not only about the evolution of the secondary palate but also about the position of the turtle in the amniote phylogenetic tree may be possible. *Emydura subglobosa* is a model of convenience because these animals were readily available from the Toronto Zoo. In addition, large clutch sizes and easy upkeep increase their favourability as a laboratory model organism and others have prepared a detailed staging table (Werneburg et al., 2009). However despite the description of the sequence of ossification contained in this paper, the authors did not examine the anatomy of the secondary palate (ie. the morphology and relationship of each palatal bone to others in the head). Furthermore only wholemount skeletal staining was used which is not sensitive enough to detect the earliest ossification centres. Therefore whole skulls were examined here using a combination of wholemount staining, micro CT and histology.

3.1.1 Wholemount staining and micro CT analysis shows that the hard palate is comprised of the palatine processes of the maxillary bones, palatine, pterygoid and vomer bones

A number of specimens were stained in wholemount to observe the chondro and dermatocranii. In the youngest specimen, the egg tooth is prominent in the external views (Fig. 3.1A). Internally, the full chondrocranium is present including Meckel's cartilage which supports the lower jaw, the interorbital septum which is the upper midline cartilage and the trabeculae cranii which connect the interorbital septum to the posterior base of the skull (Fig. 3.1B,C). In work by others it was reported that the first skull bones to ossify were the maxillary and dentary bones at stage 5 (Werneburg et al., 2009). However, we not only see the maxillary but the pterygoid is also present in our specimen so it may be slightly older than stage 5 (Fig. 3.1B,C). At stage 6 according to Werneburg et al. (2009) the majority of the other bones initiate including the angular, frontal, jugal, palatine, parietal, postorbital, premaxilla, prefrontal, pterygoid, surangular, squamosal. Thus our specimen is midway between stage 5 and 6.

The next stage examined was stage 11 and here it is possible to detect pigmentation in the skin as well as the egg tooth in the midline of the upper jaw (Fig. 3.1D). By this point all of the intramembranous bones have differentiated although the sutures have not yet fused. The gaps between the bones are especially apparent between the premaxilla, palatine and pterygoid bones (Fig. 3.1E,F). In addition the choanae or the internal nares are being circumscribed by the maxillary bones anteriorly and palatine bones posteriorly. The turtle has a unique temporal morphology with the posterior orbital rim being comprised of the post-orbital and jugal bones (Fig. 3.1E). This means that unlike the birds and squamates, the jugal bone does not project outwards from the side of the skull. This flattened morphology is typical of anapsids.

At stage 16, species specific patterns of pigmentation are visible. The snout has fully elongated with the upper jaw projecting out beyond the lower jaw (Fig. 3.1G). The skull bones have fully differentiated. The sutures have mostly fused throughout although it is still possible to see the interorbital septum between the paired palatine and pterygoid bones (Fig 3.1I). It is difficult to discern individual bones in the alizarin red stained skull. Unlike the mammalian hard palate, the choanae form a persistent communication between the oral and nasal cavities.

To better visualize the bones of the upper jaw a specimen of intermediate stage (stage 14) was examined with micro CT. Images were reconstructed and then sliced from the frontal plane. From an view in front of the skull it is possible to see the paired premaxillary bones, the maxillary and mandibular bones (Fig. 3.1J). There is a midline suture in the mandible which is also seen in squamates. Mammals however, do not have a midline mandibular suture at any stage during development of the skull. Slicing through the premaxilla the bony separation between the nasal and oral cavities is visible (3.1K). The bones comprising the anterior hard palate (anterior to the choanae) are the maxillary bone laterally and premaxillary bone in the midline. Posterior to the choanae, the hard palate is formed by the palatine bones (Fig. 3.1L) which articulate with the vomer in the midline and the pterygoid bones posteriorly (Fig. 3.1M). The vomer extends anteriorly to separate the right and left choanae. The palatal view demonstrates that the pterygoid bones also make a major contribution to the posterior hard palate and jut anteriorly to contact the vomer in the midline. Finally, the basisphenoid and basioccipital bones are in the same plane as the pterygoid and complete the bones of the hard palate.

Histology results conclude that the turtle has a bony hard palate with some of the characteristics of the mammalian (synapsid) hard palate including contributions from the

maxillary and palatine bones. There is a continuous bridge of bone across the midline composed of the premaxilla and palatine process of the maxillary bone anteriorly and the vomer, palatine and pterygoid posteriorly. However in distinction to the mammalian hard palate, in *E. subglobosa* the hard palate is considered incomplete due to the anterior openings of the choanae. The internal nares are present in this exact position in the earliest turtle found in the fossil record, *Proganochelys* (Gaffney, 1979; Carroll, 1988).

The turtle palate has similar characteristics to squamate reptiles and birds. In particular, the pterygoid forms a major part of the palate. There are some major differences as well. The main one is that the hard palate bones of the turtle are continuous across the midline whereas the squamate and bird palate is naturally cleft. In addition in squamates the epipterygoid joins the pterygoid to the maxillary bone (Boughner et al., 2007). Thus the turtle palate is a hybrid of the most primitive amniotes which have an internal nares in a similar anterior position and more modern squamate and avian reptiles which have a large pterygoid bone. To discern whether or not the turtle palatal bones are more homologous to those of mammals or to those of birds and squamates requires further ontological analysis. Based on histological data above, subsequent objectives following will be to describe the development of the turtle face in the embryo at much earlier stages when facial prominences are present.

Figure 3.1 – Wholemout skeletal staining and Micro CT of *E. subglobosa* skulls

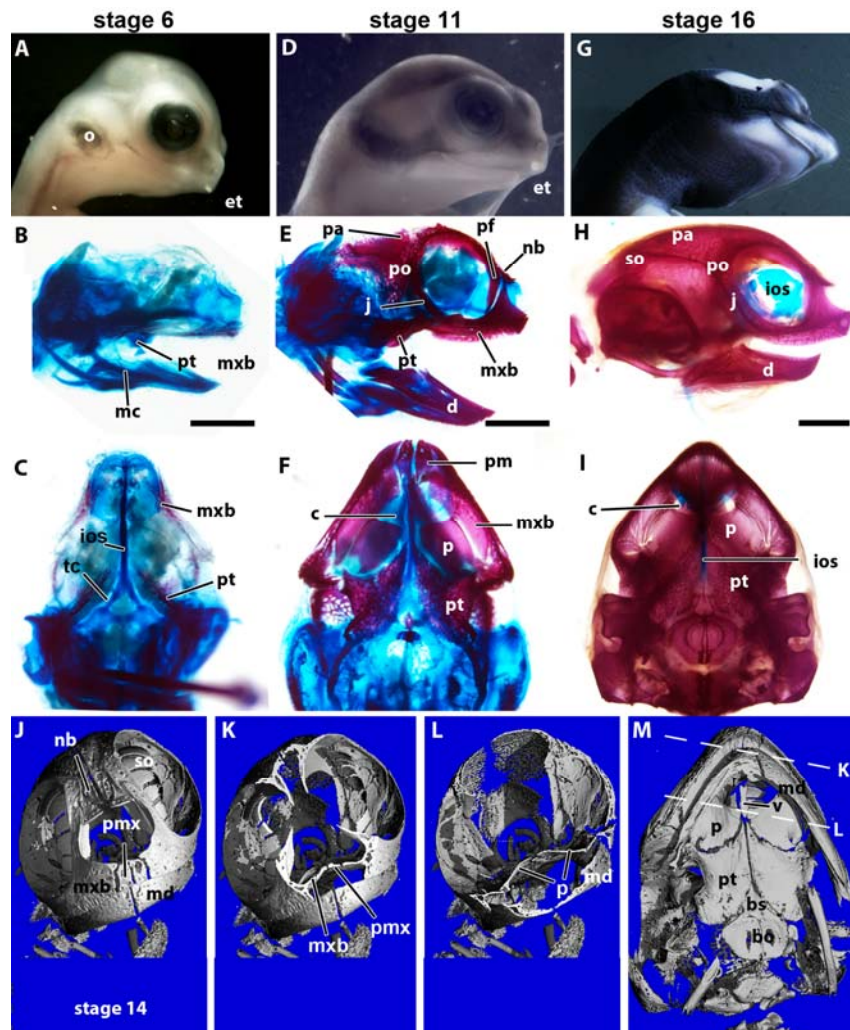


Figure 3.1. Wholemout skeletal staining and micro CT of *E. subglobosa* skulls. Stage 6 (A, B, C), stage 11 (D, E, F), and stage 16 (G, H, I) are shown in external view (A, D, G), as cleared and stained skulls (B, E, H), and in palatal view (C, F, I). At stage 6 bone condensation is minimal within the palate and the first two bones form, the maxillary and pterygoid are just starting to condense. At stage 11, the components of the palate are distinct including the choanae posterior to the premaxillary bones. At stage 16, all components of the palate seen in F have been fused together to create a continuous hard bony palate. The choanae are still present anteriorly. Micro CT of a stage 14 skull oriented at a palatal view (M) again shows the sutures have not fused between the bones of the palate. Transverse cuts show the separation of the oral and nasal cavities (J - L). Key: bo, basioccipital; bs, basisphenoid; c, choanae; d, dentary bone; et, egg tooth; ios, interorbital septum; j, jugal bone; mc, Meckel's cartilage; mx, maxillary bone; nb, nasal bone; o, otic vesicle; p, palatine bone; pa, parietal bone; pf, prefrontal bone; pm, premaxilla; po, post-orbital bone; pt, pterygoid; pt, pterygoid; tc, trabeculae cranii. Scale bars: 2mm (B same as C, E same as F, H same as I).

3.1.2 There are no palatal shelves in *Emydura subglobosa*

Histological sections of the turtle head have never been published in literature. Such data will address two major aspects of this project. First it will give not only higher resolution in sequence of bone ossification, but also pre-bone mesenchymal condensation at specific stages studied. Second, histological analysis allows for studying morphological changes in soft tissue. Stages investigated will not only include ossified embryos where bone has formed, but also the earlier stages before differentiation has occurred. We expect these earlier stages to display dynamic soft tissue changes.

My hypothesis is that since there are discrete palatine bones that span the oral cavity, there will be similar development to the mammalian secondary palate. In other words *Emydura subglobosa* forms palatal shelves and that the palatine bones ossify within the shelf mesenchyme.

We collected embryos at stage 3 which is prior to fusion of the primary palate (Fig. 3.2A-D). At the equivalent stages in mouse or chicken there are individual facial prominences and no signs of secondary palate morphogenesis. Furthermore, the chondrocranium is just initiating at this stage and only the trabeculae cranii as some of the skull base is differentiation.

Similar to other amniotes, *E. subglobosa* has a frontonasal mass, lateral nasal and maxillary prominences in the upper face (Fig. 3.2B-D). There are no signs of skeletogenic condensations with the exception of the trabeculae cranii (Fig. 3.2D). These cartilages are the first parts of the chondrocranium to differentiate in this species. In contrast, Meckel's cartilage has not yet formed in the mandibular prominences (Fig. 3.2D).

By stage 4, the primary palate has fused and this can be seen in anterior sections (Fig. 3.2E,F). The nasal slits are separated from the oral cavity in these sections (Fig. 3.2F). However more posteriorly they are reconnected (Fig. 3.2G). This opening between nasal and oral cavity will form the internal nares or choanae as was observed in our skeletal preparations. In our species of turtle, the choanae are immediately posterior to the primary palate at stage 4. As the choanae close off in more posterior sections, they choanae become shallow pits that regress till the oral roof is relatively flat. Choanae are therefore not visible in sections at section levels of the secondary palate (Fig. 3.2H, L). Mesenchymal tissue around the choanae is continuous across the oral roof, and no fusion or midline seam is observed at stages 3 to 4. The morphology of the choanae opening into the oral cavity (Fig. 3.2G) is very similar to the unfused primary

palate morphology (Fig. 3.2C) and thus can be confusing. Careful analysis of serial sections was carried out to determine which sections contained the primitive choanae. At stage 4 the chondrocranium is differentiating including the nasal septum (Fig. 3.2G,H) and Meckel's cartilage (Fig. 3.2H).

Stage 4 *E. subglobosa* embryos are predicted to have incipient palatal shelves. These are visible in a chicken embryo of an equivalent stage (chondrocranium present in stage 30 chicken embryos (Ashique et al., 2002b). In the mouse after fusion of the primary palate, palatal shelves grow outwards from the medial surfaces of the maxillary prominences (E12.5) and this is just at the time when cartilages are beginning to condense. Surprisingly, palatal shelves were not detected in serial sections through the head of *E. subglobosa* (Fig. 3.2F-H).

To rule out a later appearance of palatal shelves we also analyzed serial sections of stage 5 *E. subglobosa* embryos (Fig. 3.2I). At this time, mesenchymal condensations for the maxillary and dentary bones were present (Fig. 3.2J). Picrosirius red staining is a more sensitive method of detecting early bone condensation than wholemount staining.

Once again there were no palatal shelves just posterior to the choanae where we know from our wholemount staining the palatine bones will subsequently form according to wholemount skull staining results (Fig. 3.2J-M). Indeed the very early condensations for the palatine bones were visible posterior to the choanae (Fig. 3.2K). In other words, palatine bone condensations were located in sections cut through the most posterior outpocketing of the choanae where there is no longer a connection between nasal and oral cavities (Fig. 3.2K). These bones were differentiating directly in the mesenchyme between the nasal and the oral cavity. This is in contrast to birds, squamates and mammals where palatine bones form within the palatal shelves.

Figure 3.2 – Histology of the developing primary and secondary palate in *E.subglobosa*

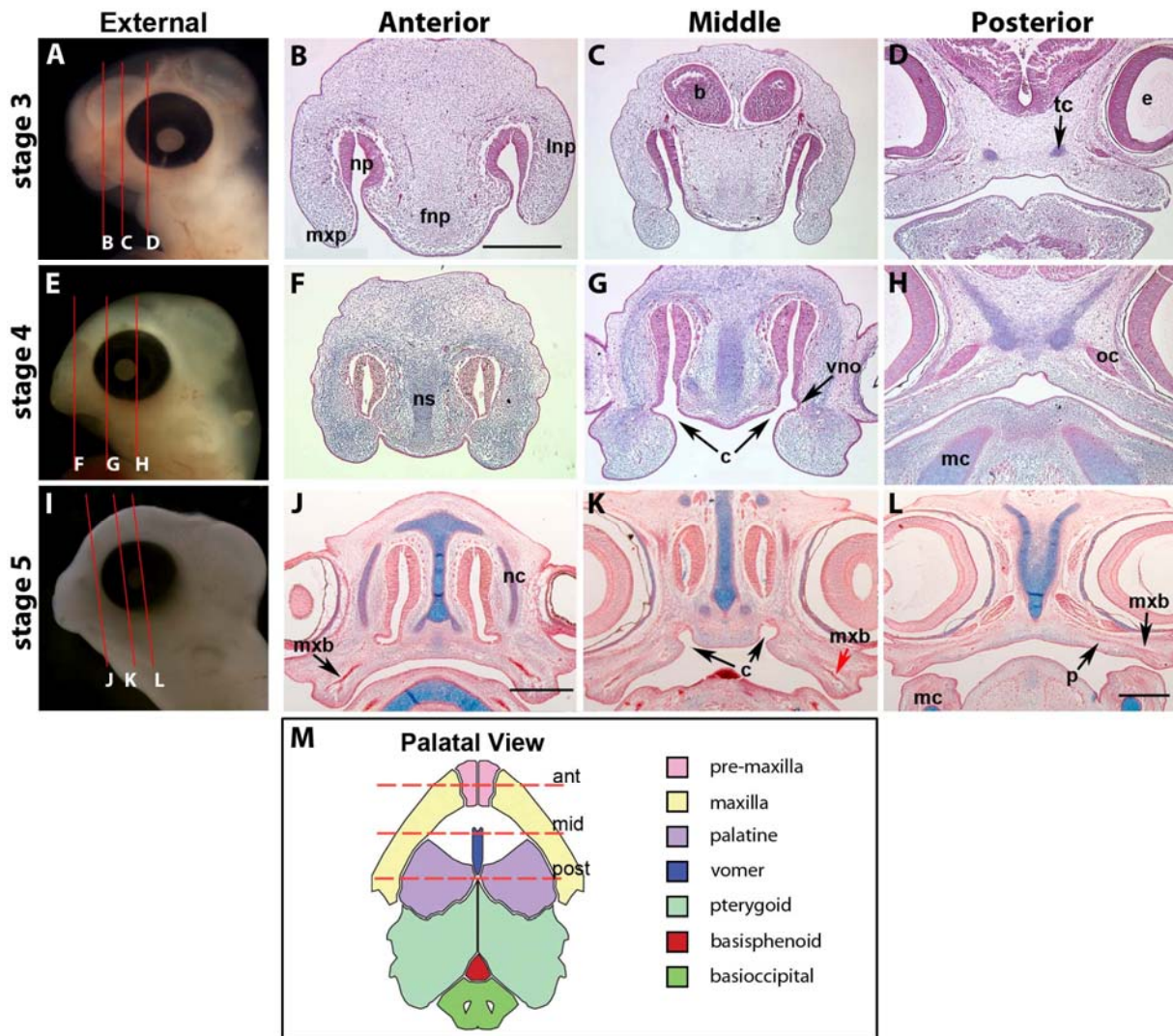


Figure 3.2. Histology of the developing primary and secondary palate in *E. subglobosa*. Embryos at stage 3, 4 and 5 were sectioned in the transverse plane. Planes of section are indicated in lateral views of whole embryos (A, E, I). Three representative planes of section are shown, anterior to the choanae (B,F, J), middle or within the choanae (C, G, K), and posterior to the choanae (D, H,L). Unfused facial prominences are present at stage 3 (A-D) whereas at stage 4 the primary palate has fused (E-H). Bone condensation is first detected at stage 5 (I-L). Palatal shelves are normally evident in other amniotes such as mice and chicken at the equivalent to stage 4 in turtles. Surprisingly, there is no evidence of medial outgrowths from the maxillary prominence, posterior to the primitive choanae (F, G). These are also not present at stage 5 (J-L). However at stage 5 maxillary (J-L) and palatine bone (L) condensations can be detected. Note the medial location of the palatine bone condensation (black arrowheads, J) and the lateral maxillary bone condensations (red arrow, J). (M) Cartoon of *E. subglobosa* palate at stage 14 which provides a reference for the depth of transverse sections. Key: b, brain; c, choanae; e, eye; fnp, frontonasal prominence; lnp, lateral nasal prominence; mc, Meckel's cartilage; mxp, maxillary prominence; np, nasal pit; ns, nasal septum; oc, optic chiasma; tc – trabeculi cranii; vno, vomeronasal organ. Scale bars: Bar in B = 220 μ m and applies to B-D, F-H; Bar in J = 500 μ m and applies to J, K; Bar in L = 500 μ m.

3.2 Cellular dynamics

Wholemout staining shows that palatine bones are a component of the hard palate of *E. subglobosa*. However, when studying earlier stages of development, it was discovered that palatal shelf formation did not occur. Thus instead of palatine bone differentiating within palatal shelves, direct condensation of bone was carried out between the nasal and oral cavities. As the literature has never described such a developmental process, an investigation into possible mechanisms for the failure of palatal shelf budding from the maxillary prominences was carried out. By mapping patterns of cell apoptosis and proliferation, corresponding results will give insight into understanding the cellular dynamics within the maxillary prominence.

The driving hypothesis in this aim was that the medial side of the maxillary prominence does not initiate palatal shelf formation due to an increase in apoptosis. In other words, these experiments in cellular dynamics will test whether there were rudimentary palatal shelf outgrowths which then regressed due to apoptosis. The second or alternative hypothesis is that proliferation is even across the maxillary prominence which prevents outgrowth of the medial side.

3.2.1 Apoptosis is not increased on the medial side of the maxillary prominence

Cell apoptosis was investigated at stages 3 and 4 of *E. subglobosa* using the TUNEL assay. At stage 3, the primary palate is fusing and the primitive choanae have not yet formed whereas at stage 4 the primitive choanae are present. In both anterior (anterior palate, Fig. 3.3A,C) and posterior (secondary palate, Fig. 3.3B,D) sections, there were very few apoptotic cells. Positive cells were found in the nasal pit epithelium close to the fusion zones (Fig. 3.3A,C). However posterior to the choanae, there were almost no detectable apoptotic cells except in the optic chiasm (Fig. 3.3B,D). Importantly, no apoptosis was observed at the medial edges of the maxillary prominences nor anywhere else in the embryonic face of *E. subglobosa*. These results reject the first hypothesis, that an increase in apoptosis underlies the lack of palatal shelf formation.

3.2.2 Cell proliferation is not decreased on the medial side of the maxillary prominence.

As an embryo grows, there is active cell proliferation in the undifferentiated mesenchyme (McGonnell et al., 1998; Szabo-Rogers et al., 2008; Higashihori et al., 2010). In order for budding to occur it is necessary for one region to maintain this high level of proliferation while the adjacent region drops the level of proliferation. This mechanism has been described for the maxillary prominences where the proliferation rate in the roof of the stomodeum drops more rapidly than the proliferation of the chicken maxillary prominence (Minkoff and Kuntz, 1978). Within the maxillary prominence mesenchyme there have been reported only slight differences in proliferation from medial to lateral in the chicken embryo in one study (McGonnell et al., 1998) whereas in another study there are lower rates of proliferation in the centre of the maxillary prominence (Bailey et al., 1988). Here this study will focus on the maxillary prominence and any proliferative patterns that may help explain the lack of palatal shelf formation in *E. subglobosa*.

Cell proliferation was analyzed at stages 3 and 4. These stages were selected as to cover stages when it was likely that proliferation differences might be seen that could set up differential outgrowth of the palatal shelves. These stages are equivalent to approximately stage 22 and 27 in the chicken embryo. An overall impression of the proliferation patterns at stage 3 and 4 will first be described. At stage 3, the primary palate plane had more proliferative cells aggregated towards the lateral edges of the frontonasal mass whereas the centre, where the nasal septum will form has much lower proliferation (Fig. 3.3E). The same pattern is observed in more posterior sections (Fig. 3.3F). There is high proliferation in the lateral nasal prominences (Fig. 3.3E). In stage 3 anterior sections, only the most cranial part of the maxillary prominence was included (Fig. 3.3E). In posterior sections there is high proliferation in the maxillary prominence mesenchyme (Fig. 3.3F).

Once the primary palate has fused at stage 4, proliferation is still strong along the lateral edges of the frontonasal mass and in the lateral nasal prominences (Fig. 3.3G). Regions of decreased proliferation are observed in the midline of the frontonasal mass in both the primary palate and in the region of the primitive choanae (Fig. 3.3G,H). Proliferation in the maxillary prominences is again difficult to observe in the shallow anterior section but can be seen better in

the deeper posterior sections (Fig. 3.3H). There appears to be lower proliferation in the centre of the maxillary mesenchyme.

To quantify the proliferation in different regions of the maxillary prominence, the posterior sections of stage 3 and 4 *E. subglobosa* embryos were analyzed in more detail since this is where palatal shelves are expected to be budding out (Fig. 3.3F, H, see boxes for area of section analyzed). The maxillary mesenchyme was divided into six areas for cell counting. Each area was estimated to include similar total cell numbers and the percentage of proliferative cells in each region was calculated.

At stage 3 there were significant differences between areas 1 (upper medial maxillary, 25%) and 2 (upper middle maxillary, 15%). Differences between area 4 (lower medial maxillary, 25%) and 2 (upper middle maxillary) were also significant (Fig. 3.4). It is interesting that these same differences were observed in stage 4 *E. subglobosa* and were slightly more pronounced (Fig. 3.4).

Quantitative analysis by cell counts displays a significant increase in proliferation at the medial edges of the maxillary prominence when compared to middle regions. This pattern of increased proliferation under the epithelium is similar to what has been reported for the chicken embryo (Bailey et al., 1988). Despite these similarities to the chicken, *E. subglobosa* does not form even rudimentary palatal shelves whereas the chicken does. A possible explanation may be that although there is higher medial proliferation, this level is not markedly high enough to initiate palatal shelf budding. Lack of shelf formation may also be explained by an insufficient decrease in proliferation at non-growth regions, leading to more even distribution of proliferating cells and an even expansion of the prominence increase instead of lateral budding.

Since the data collected is from two stages, these proliferation results rule out the presence of initially high levels of proliferation which then decrease, preventing shelf outgrowth. Our data supports that from stage 3 (before shelf formation) till stage 4 (when shelves should have already formed), the relatively higher peripheral proliferation rate is maintained. Since cell proliferation patterns are constant throughout this developmental time period, this does not support the hypothesis of vestigial shelves that failed to develop further.

Figure 3.3 Cellular dynamics in the developing *E. subglobosa* palate

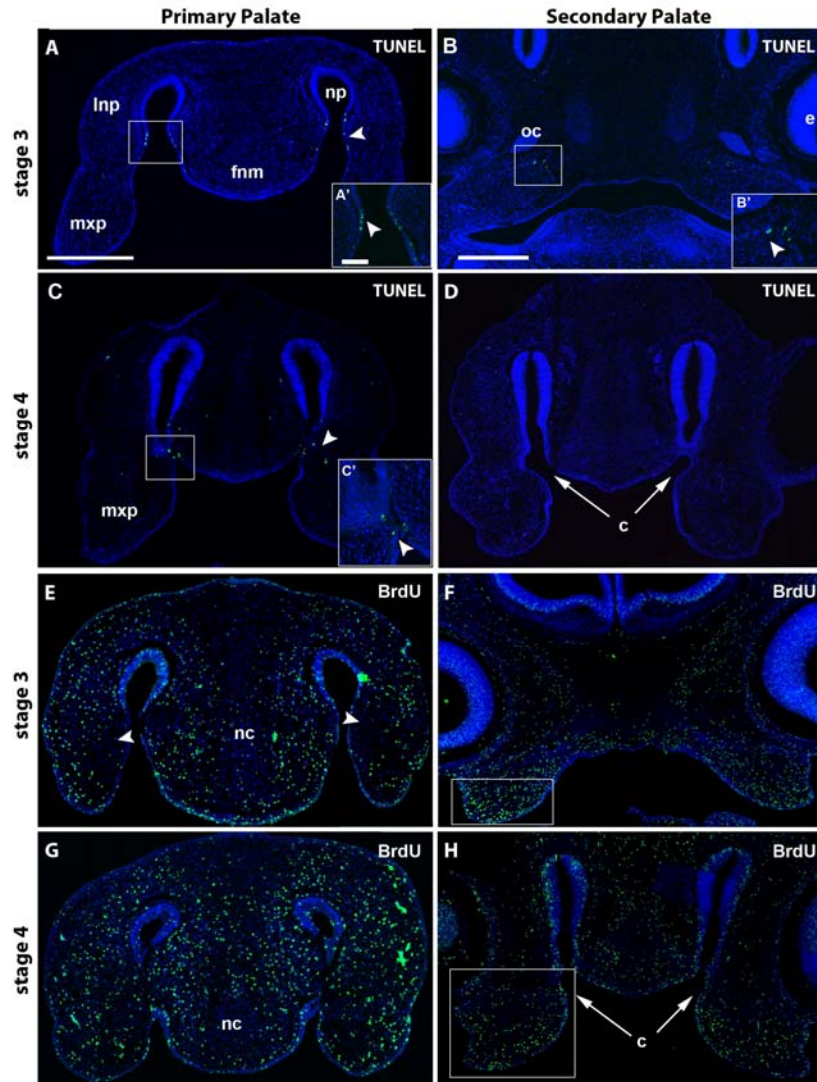


Figure 3.3. Cellular dynamics in the developing *E. subglobosa* palate. Transverse sections of the head stained for apoptotic (A-D) and proliferating cells (E-H). Apoptotic are detected in the nasal slit epithelium close to the fusion zone between the frontonasal mass and maxillary prominences (A' and C', arrowheads). Posteriorly, apoptotic cells are observed under the optic chiasma (B' arrowhead). No apoptotic cells are observed in the area where the primitive choanae open into the oral cavity (D). E) Less proliferative cells are seen in the cartilage condensation of the nasal septum as well as the medial edges of the maxillary prominences (arrowheads in E). Posteriorly, where palatal shelves are predicted to form, maxillary cell proliferation seems constant except for the central mesenchyme, most distant from the surface epithelium. Boxed maxillary regions (F and H) were analyzed quantitatively. Key: b, brain; c, choanae; e, eye; fnm, frontonasal mass; lnp, lateral nasal prominence; np, nasal pit; mxp, maxillary prominence; mc, Meckel's cartilage. Scale bars = 400 μ m for low magnifications and 100 μ m for insets.

Figure 3.4 – BrdU data in graphical format

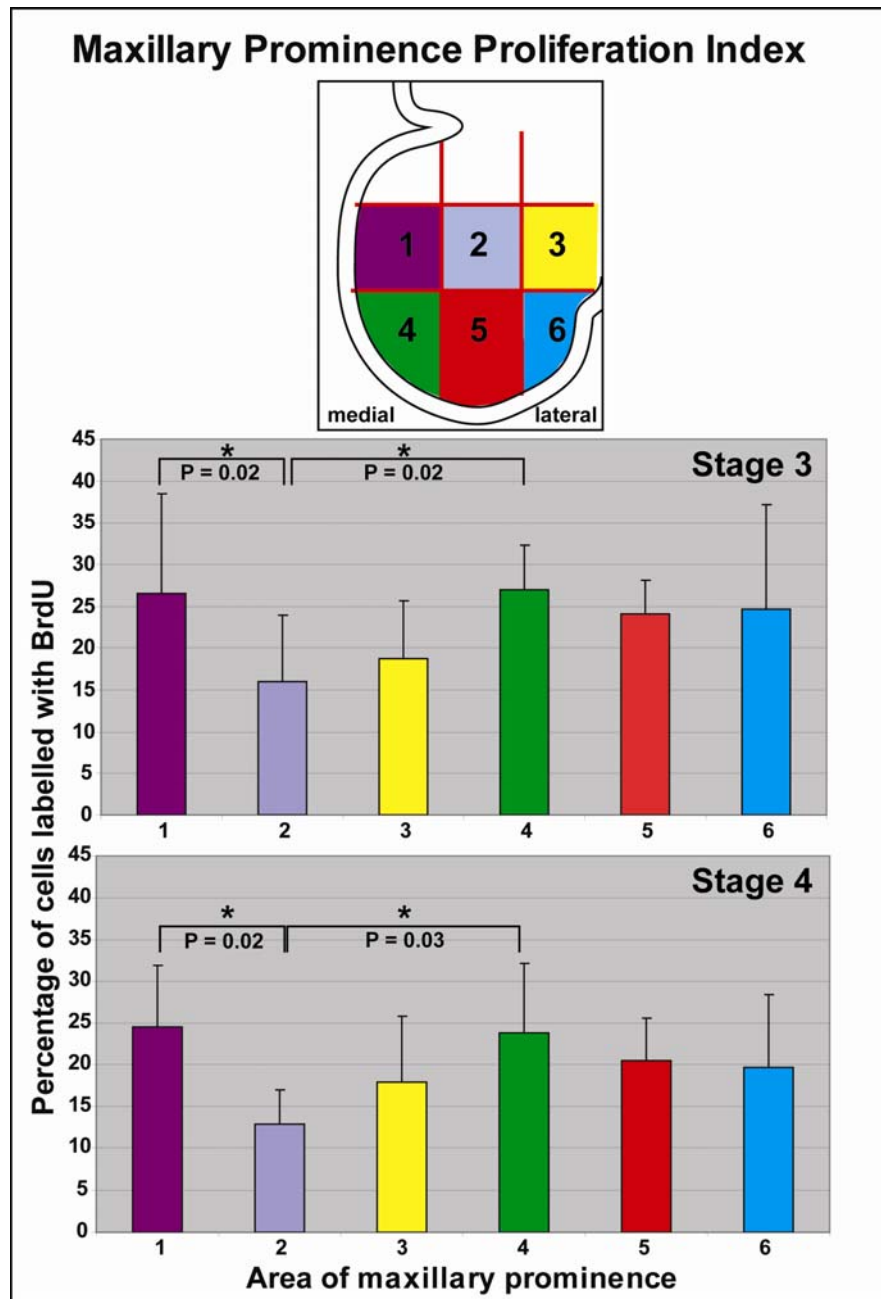


Figure 3.4. Quantitative BrdU data in graphical format. Maxillary prominence at secondary palate depth is divided into 6 parts (areas 1-6) to count percentage of proliferative cells. In both stage 3 and 4, statistical significance was reached between areas 1 and 2 as well as 2 and 4; that is, the medial and lateral regions of the maxillary prominence have greater proliferation than regions deep in mesenchymal tissue, away from the epithelium. Tukey's post-hoc testing of one-way ANOVA was used to generate p values.

3.3 Gene expression in the embryonic turtle face

The histological analysis showed very clearly that palatal shelves do not grow out from the maxillary prominences. Therefore the roof of the oral cavity is on the opposite side of the nasal cavity. In consideration of these results, the next hypothesis postulated was that the roof of the oral cavity of *E. subglobosa* is similar to the primitive oral cavity in mammals, before palatal shelves form. In order to test this hypothesis I examined expression of a panel of genes that are present in the epithelium of the primitive stomodeum of mammals. A second hypothesis is that similar signaling pathways are at work in the morphogenesis of the turtle palate compared to those used in other vertebrates. The third hypothesis of this section was that birds are more closely related to turtles than mammals, thus the gene expression patterns of the chicken maxillary prominence and palate would resemble those of *E. subglobosa*.

3.3.1 Expression of *Bmps* during palate morphogenesis

Bone Morphogenetic Proteins (*Bmps*) are required for maxillary prominence morphogenesis and when *Bmpr1a* is conditionally deleted, cleft lip and palate is induced in mice (Liu et al., 2005). In addition *Bmp7* is strongly expressed in the stomodeal epithelium prior to palatal shelf formation in the mouse (Hu and Marcucio, 2009b) and in the chicken (Ashique et al., 2002a; Foppiano et al., 2007; Hu and Marcucio, 2009b). *Bmps* are also involved in intramembranous bone formation (Barlow and Francis-West, 1997).

In order to map expression of *Bmp2*, *4* and *7* I cloned parts of the open reading frames of *Bmp2* and *Bmp7* were cloned (Table 1) and *Bmp4* from another species of turtle (*Trachemys scripta*, sequence ID: AAR3824.2) was obtained. Primary stages of focus were on stage 3, prior to fusion of the primary palate and stage 4 after fusion and prior to differentiation of intramembranous bones. At stage 3, *Bmp2* transcripts (Fig. 3.5A-E') are primarily restricted to the epithelium of the frontonasal and maxillary prominences in both anterior (at primary palate level, Fig. 3.5A,A') and posterior sections (secondary palate level; Fig. 3.5B,B'). Maxillary expression is interestingly restricted to the cranial and medial regions close the zone of contact with the frontonasal mass (lip fusion zone, Fig. 3.5A'). In addition the epithelium of the nasal slits expresses *Bmp2* but at low levels (Fig. 3.5A'). Expression is similar at stage 4 with

transcripts being present in the stomodeal epithelium (Fig. 3.5C'-E'). There are foci of strong expression in the posterior choanae epithelia (Fig. 3.5E').

More similar to *Bmp7*, *Bmp4* (Fig. 3.5F-J') is expressed in both epithelial and mesenchymal tissue at the lateral edges of the frontonasal mass in the primary palate (Fig. 3.5F,F'). Interestingly, concentrated transcript expression is also observed in the groove between the lateral nasal and maxillary prominence in stage 3 *E. subglobosa* (Fig. 3.5F'). Deeper sections of the same embryo reveal that there is strong expression of *Bmp4* in the medial epithelium of the maxillary prominences and stomodeum (Fig. 3.5G'). At stage 4 expression strengthens at the caudal edge of the frontonasal mass (Fig. 3.5H') and is concentrated in the posterior ends of the choanae epithelia overlapping *Bmp2* (compare Fig. 3.5I' to E'). There is also expression of *Bmp4* in the mandibular epithelium and olfactory epithelium at stage 4 (Fig. 3.5J').

Similar to *Bmp2*, *Bmp7* expression (Fig. 3.6A-E') is present in the stomodeal epithelium at stage 3 (Fig. 3.6A'). Unlike *Bmp2*, there is also mesenchymal expression in the cartilage of the nasal septum and in future sites of intramembranous bone formation in the maxillary prominences (Fig. 3.6A',B'). In stage 4 embryos, *Bmp7* is abundant in the cartilage of the nasal septum (Fig. 3.6C',D'). This is similar to what has been observed in chicken embryos (Ashique et al., 2002b). There is strong expression in the respiratory epithelium at stage 4 (Fig. 3.6C', D') again a pattern that is also conserved with chicken (Ashique et al., 2002a). The epithelium and mesenchyme of the posterior end of the choanae have overlapping, and strong expression of all three *Bmps* (Fig. 3.5E', I'; 3.6E'). This stomodeal epithelial expression of *Bmps* in turtle is similar to the primitive oral epithelium of the chicken prior to formation of the unfused secondary palate as well as the mouse embryo prior to E12.5 (Francis-West et al., 1994; Ashique et al., 2002a; Foppiano et al., 2007; Hu and Marcucio, 2009b).

Table 3.1 DNA sequences of *E. subglobosa* cloned fragments.

<i>Bmp2</i>	GGCGATTGGGCCCCGACGTCGCATGCTCCCGGCCGCCATGGCGGCCGCGGGAATTCGATTGGATGTCTTTTG CAACTGGATTTGTGGCGTTTGGCGTGTGTGTTTGGCTTGGCGTTTCTCTCTTATGGAGAGGGTGTCCCTTGC CATCATGGCTAAAAGTTACTAACAATGGCCTTAGCTGAGACCAGCTATCTTCATCCTGATGCAAAGAGCGGC TAATCCTAACATGCCTCTTGGAACACTGCTCTCATTTGTCCAAGTGAACCACTCTACTACAAACCCATGATT AGGCTGTCTATGTGCAATCCACCTCATTACAGCTGGTGTTACATCAAAGCTTTCCCATTTACTTGCATTCTGA TGCACCAACCTGGTGTCCAAAAGTCTTGTGGCAGGGTCCCTAGAAGAAGCTGTGGCTGGCTTTATAATTTCA TAAATATTAATACGGTGATGATAGCTGCTATTGTTCTCAAAGGCTGCCTGCACCTGCTCCCGAAAAATCTGA AGTTTCAGCCGAGGTGAGAACTCCTCATTAGGGATGGAAGTTAAATTAAGAAGAAACGCCGTGCTAATCA CTAGTGAATTCGCGGCCGCTGCAGGTCGACCATATGGGAGAGCTCCCAACGCGTTGGATGCATAGCTTGAG TATTCTATAGTGTACCTAAATAGCTTGGCGTAATCATGGTCATAGCTGTTTCTGTGAAATGTTATCCG CTCACAAATTCACACAACATACGAGCCGGAAGCATAAAGTGTAAGCCTGGGGGTGCCTAATGAGTGAGCT AACTCACATTAATTGCGTTGCGCTCACTGCCCGCTTTCAGTCGGGAAACCTGTCGTGCCAGCTGCATTAA TGAATCGGCCAACGCGCGGGGAGAGCGGTTTGCCTATTGGGCGCTCTTCCGTTCTCTCGCTCACTGACTCG CTGCGCTCGGTCTGTCGGCTGCGGCGAGCGGTATCAGTCACTCAAGGCGTAATACGNTNATCCACAGAAT C
<i>Bmp7</i>	ACAGGACAGCAACTTCCTGACTGAGGCGGACATGGTCATGAGCTTCGTGAATCTGGTGGAGCATGACAAAG AGTTCCATCATCAGCGCTATCACCATCGGGAGTTTCAGGTTTGATCTCTCCAGAATCCAGAGGGGGAAGCAG TGACTGCTGCTGAGTTCAGGATATATAAGGATTACATCCGAGAACGGTTTGATAATGAAACATTCCAGATAA GCGTCTACCAAGTACTGCAGGAGCACCCAGGAAGGGATTTCAGATTGTTCCCTGTGACACTCGAACAATTT GGGCTGCAGAAGAAGGTTGGTTGGTGTGTTGATATTACAGCAACCAGTAATCTCTGGGTGGTAAATCCACAAC ATAATCTCGGTCTGCAGCTATCAGTTGAGAGTATAGATGGACAAAGCATCAATCCCAAACCTGGCTGGTCTAA TCGGAAGACATGGCCACAAAATAACCAGCCTTTCACGGTAGCATTCCTCAAAGCCACAGAAGTGCATCTCC GCAGTATTCGTTCCNCGGGANGNAAACAAAGGANCCAGATTTCGATCGAAAA
<i>Fgfr2</i>	ACTATCTGACCTGGTGTCTAGAGATGGAGATGATGAAAATGATTGGGAAGCACAAAAATATTATCAATCTTCT TGGAGCCTGTACACAGGATGGTCCATTGTATGTGATAGTTGAATATGCTTCTAAAGGGAATCTGCGGGAGTA CCTTAGAGCACGGCGACCCCTGGAATGGAATATTCATTTGATATCAACAGGGTACCGGAAGAGCAGATGA CATTCAAAGACTTAGTATCATGACATACCAACTGGCAAGGGCATGGAATACCTGGCTTCACAGAAATGCA TTCATCGAGATTTAGCAGCAAGAAATGTTTGGTGAAGTAAATGTGATGAAAATAGCAGACTTTGGTT TGGCCAGAGACATCAACAATATAGATTATTAAAAAGACTACTAATGGCCGGCTGCCTGTAAAGTGGATG GCTCCAGAAGCCCTATTTGACAGAGTTTACACACATCAAAGTGATGTTTGGTCAATTTGGTGTGTTGATGTGGG AGATCTTCACTTTGGGAGGATCACCTATCCAGGAATTCCAGTGGAGGAACTTTTAAGCTGCTTAAAGAAG GGCAGAAATGGATAAGCCTGGCCA
<i>Ptch1</i>	CCTGGAGCATGTTCGCGCCAGTGTTAGATGGAGCTGTGTCTACTCTGCTTGGAGTGTTAATGCTTGCAGG GTCCGAGTTTGATTTATTGTAAGGTATTTCTTTGCTGTTTGGCAATTTTAACCATCTGAGGAGTTCTGAATG GATTGGTGTCTGCTTCAGTTCCTTCTGTCTTCTTTGGACCATATCCTGAGGTTTCTCCAGCCAATGGACGGAA CAGATTGCCTACTCCCTCTCCTGAGCCAGCTCCTANCGTTGTGAGGTTTGCACTGCCACCTGGACACACAAAT AATGGATCAGATTCTGTCTGATTCTGAGTACAGTTCTCAGACCACAGTGTGAGGAATCAGTGAGGAACCTCCAT CAATACGAGGTCACTCAGAGCTCTGGTGCACCTGTCCACCAAGTAATAGTGGAAAGCAACTGAGAATCCTGTC TTTGCCAGATCCACTGTGGTTACGCCAGAGACAAGATATCATCAGCCAAGTCCAAAATTACAACTAACCCA GAAGCTGGGTCCCAGCAGACGTGGCATCATAACAGACAACCTANACAGGAATTGAGGGAAGGACTACGACC ACCTCCTTACAGGCCACGCAGGGATGCTTTGAAATTTCTACTGAAGGGCATTCTGGACCTAGCTCTAGGGA CCGCTCGAGCCATAGGACTCGTTCTCATAACATTAGAAGCCCAGCATTCACTGCCATGGGTGCTTCAGTGCC AGCATACTGCCNACCTATCACCACCGTGACCGCCAATCACTAGTGAATTCGCGGCCGCTGCAGGTCGACCA TATGGGAGAGCTCCCAACGCGTTGGATGCATAGCTTGAGTATTCTATANTGTACCTAAATANCTTNGNGTA ATCATGGNCATAG CTGTTTCTG

Figure 3.5 – *Bmp2* and *Bmp4* Gene expression of *E. subglobosa* stage 3 and 4.

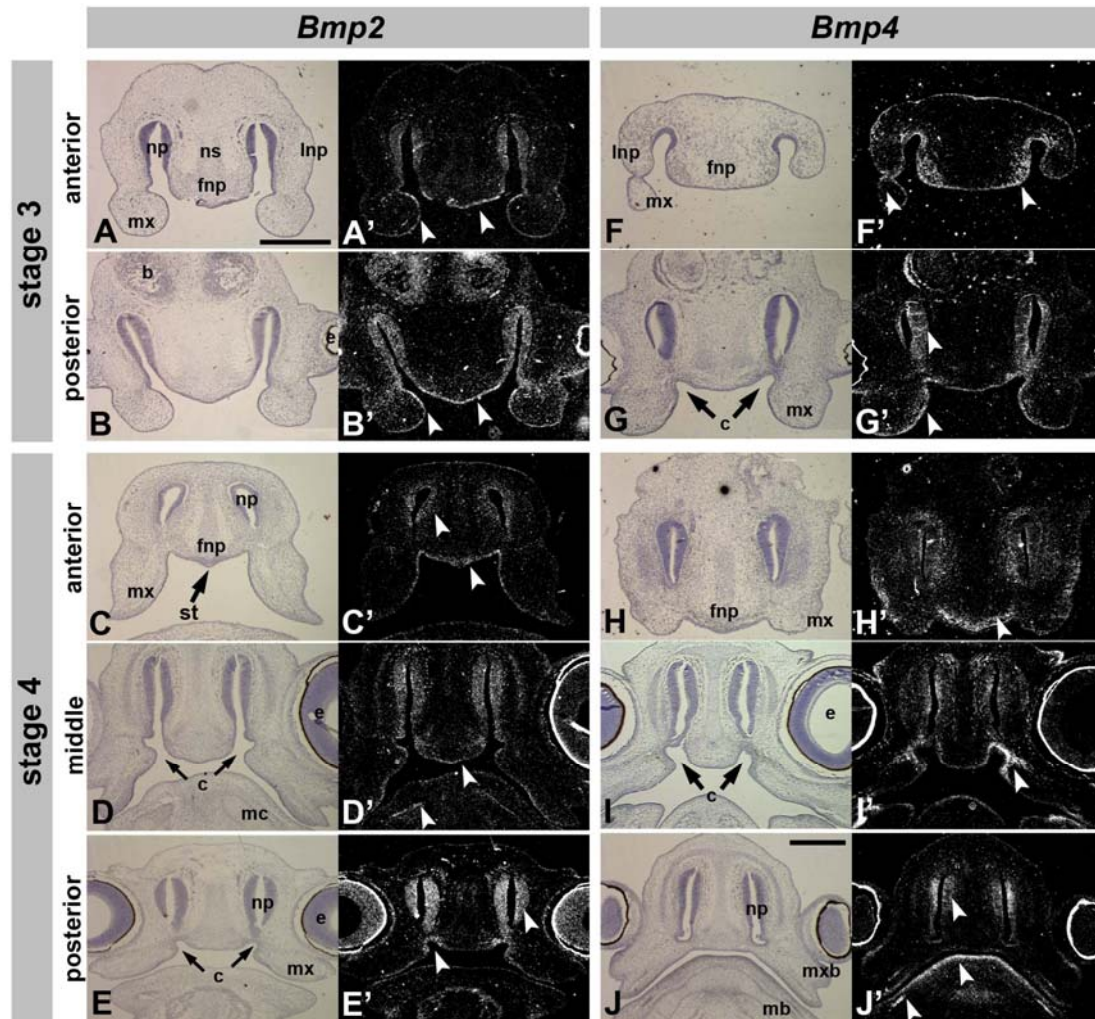


Figure 3.5. *Bmp2* and *Bmp4* gene expression in the stage 3 and 4 embryo in the primary and presumptive secondary palate.

Transverse sections through primary palate (anterior) and presumptive secondary palate (middle and posterior) of *E. subglobosa* at stages 3 (A, A', B, B', F, F', G, G') and stage 4 (C, C', D, D', E, E', H, H', I, I', J, J'). Radiolabeled *in situ* hybridization was carried out and white silver grains in darkfield images (A', B', C', D', E', F', G', H', I', J') show the location of gene transcripts. *Bmp2* is expressed in the epithelium of the frontonasal and maxillary prominences near sites of primary palate fusion (arrows, A') and in the stomodeal epithelium (arrows, B'). At stage 4 there is stronger expression in the nasal pit (C' upper arrowhead, D', E'). *Bmp2* is also in the stomodeal epithelium (D', upper arrowhead), perichondrium of Meckel's cartilage (lower arrowhead, D') and in the choanae invaginations (lower arrowhead, E'). *Bmp4* is located in mesenchyme lateral and medial to the nasal pit at stage 3 (arrowheads F'). Posteriorly, *Bmp4* is localized to the oral epithelium of the maxillary prominence extending into the choanae invaginations (lower arrowhead G'). By stage 4, *Bmp4* expression is strong in the frontonasal prominence (H', arrowhead) and robust in the choanae (I', arrowhead). *Bmp4* is also present in the nasal epithelium, mandibular oral surface, and early condensing bone (arrowheads J'). Key: mx, maxillary prominence; np, nasal passage; ns, nasal slit; fnp, frontonasal prominence; lnp, lateronasal prominence; b, brain; st, stomodeum; c, choanae; e, eye. Scale bars: 500 μ m. Scale bar in A applies to A - I'. Scale bar in J applies to J and J'.

Figure 3.6 – *Bmp7* and *Ptch1* Gene Expression of *E. subglobosa* stage 3 and 4.

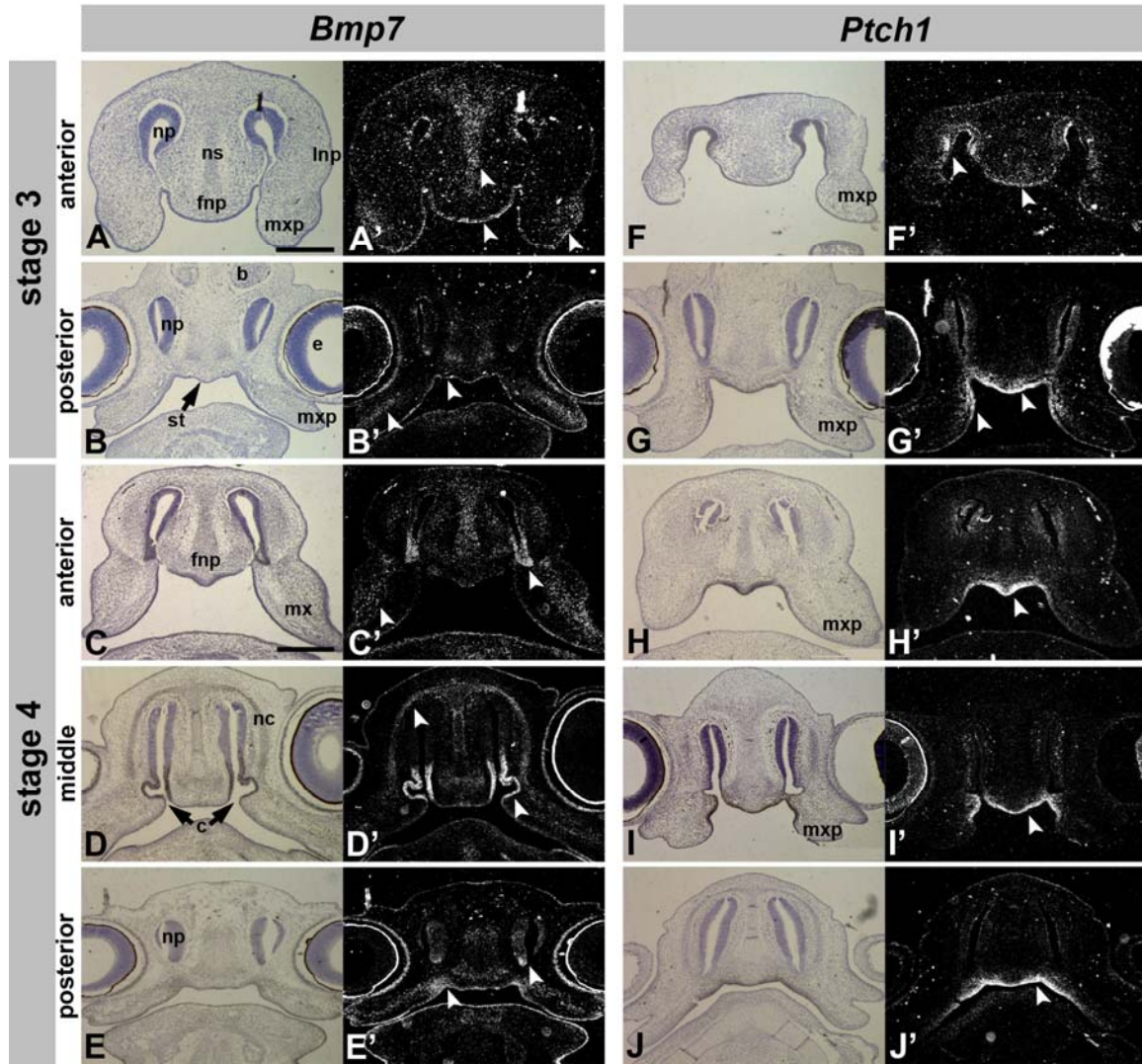


Figure 3.6. *Bmp7* and *Ptch1* Gene Expression of *E. subglobosa* stage 3 and 4.

Transverse sections through primary palate (anterior) and presumptive secondary palate (middle and posterior) of *E. subglobosa* at stages 3 and stage 4. Early *Bmp7* expression at stage 3 is located in the nasal cartilage, oral epithelium of frontonasal and maxillary prominences, and lateral mesenchyme of maxillary prominence (A' and B', arrowheads). Stage 4 *Bmp7* expression is restricted to the respiratory epithelium of the nasal cavity (C', D', arrowheads). It is also expressed in the oral epithelium of the entire oral cavity, the nasal septal cartilage, mesenchyme of the maxillary and mandibular prominences (D', E'). *Ptch1* expression is strongly restricted to epithelium and mesenchyme of the stomodeal roof and medial maxillary prominences at stage 3 (F' and G' arrowheads). This expression persists into stage 4 and across the three planes studied (H', I', J' arrowheads). Key: np, nasal passage; fnp, frontonasal prominence; ns, nasal septum; mxp, maxillary prominence, lnp, lateral nasal prominence; b, brain; st, stomodeum; nc, nasal capsule; c, choanae. Scale bars: 500 μ m; A applies to A', B, B', F, F', G, and G'; bar in C applies to C', D, D', E, E', H, H', I, I', J, and J'.

3.3.2 Expression of *Shh* and *Fgf* pathway genes

The Sonic Hedgehog signaling pathway is also active during facial morphogenesis and is required for setting up the boundary between facial and oral ectoderm (Hu et al., 2003; Marcucio et al., 2005; Hu and Marcucio, 2009a). One of the receptors for Shh, Patched, is not only a mediator of the pathway but also a direct target. The Richman lab has shown in other reptile work that *Ptch* expression is increased in the presence of SHH protein and that when Hh signaling is blocked with cyclopamine *Ptch* expression is eliminated (Handrigan and Richman, 2010).

A fragment of the *E. subglobosa* orthologue of *Ptch1* was cloned and its expression patterned examined in stage 3 and 4 turtle embryos (Table 1, Fig. 3.6F-J'). In stage 3 there are transcripts surrounding the nasal pits in both epithelium and mesenchyme (Fig. 3.6F'). In posterior sections, expression is also observed in the nasal epithelia, across the presumptive oral roof and on the medial surfaces of the maxillary prominences (Fig. 3.6 G').

In stage 4 embryos *Ptch* continues to be highly restricted to the caudal edge of the frontonasal mass (Fig. 3.6H'). Further posteriorly, the epithelium and adjacent mesenchyme lining the roof of the oral cavity express high levels of *Ptch1* (Fig. 3.6I', J'). Thus similar to chicken embryos *Ptch1* expression marks the primitive oral epithelium (Hu and Helms, 1999; Marcucio et al., 2005). In the oral epithelium of the more advanced mammalian secondary palate, *Shh* and *Ptch* expression are restricted to the rugae (Rice et al., 2006).

Expression of two genes in the FGF (Fibroblast growth factor) pathway was examined that would indicate areas with higher FGF signaling activity (Fig. 3.7A-J'). One is the receptor for several epithelial FGFs, *Fgfr2* (receptor for FGF2, 4 and 18 (Ornitz et al., 1996) and the other is *Sprouty2*, a pathway mediator and a direct target of the FGF signaling pathway (Minowada et al., 1999). Here we obtained a clone for *Trachemys scripta* for *Spry2* (J. Moustakas, not entered in NCBI) and cloned a portion of *Fgfr2* coding sequence for *E. subglobosa* (Table 1).

At stage 3, the receptor for FGF, *Fgfr2* is not as abundantly expressed as the other genes examined. However there is some light signal in the oral epithelium and caudal

edge of the frontonasal mass epithelium (Fig. 3.7A'). There is mesenchymal expression in the maxillary mesenchyme in two horizontal stripes that line up with the maxillo-lateral nasal groove. (Fig. 3.7B'). At stage 4 expression of *Fgfr2* is stronger than at stage 3. Anterior to the choanae, there is strong expression in the caudal frontonasal mass epithelium and in the nasal passages (Fig. 3.7C'-E'). There is also expression of *Fgfr2* in the medial maxillary epithelium (Fig. 3.7C'). At the level of the choanae, there is weak expression in the epithelium of the choanae and medial surfaces of the maxillary prominences (Fig. 3.7D'). Posterior to the choanae, there a similar medio-lateral stripe of *Fgfr2* expression beneath the eyes (Fig. 3.7E') as was visible at stage 3. Unlike in the chicken where *FGFR2* is strongly expressed in cartilage condensations (Wilke et al., 1997), in *E. subglobosa* there is no expression in the frontonasal, nasal septal and Meckel's cartilage (Fig. 3.7C'-E').

The expression of *Spry2* expression in stage 3 embryos is restricted to frontonasal and lateral nasal mesenchyme closest to the nasal epithelia (Fig. 3.7F'). At this depth, there is no detectable *Spry2* transcript in both mesenchymal and epithelial components of the maxillary prominences (Fig. 3.7F'). This is in stark contrast to a similar stage chicken embryo which has abundant expression in the caudal half of the maxillary prominence, adjacent to *Fgf8*-positive epithelia (Szabo-Rogers et al., 2008). However, in more posterior sections, there is very strong *Spry2* expression in oral surfaces of the maxillary prominences in both epithelium and mesenchyme (Fig. 3.7G'). This expression is also observed in lateral mandibular tissue (Fig. 3.7G').

At stage 4 similar expression patterns are observed for both *Spry2* and *Fgfr2*. Anterior to the choanae, there is strong expression of *Spry2* the caudal frontonasal mass epithelium and in the nasal passages (Fig. 3.7H', I'). In the chicken, *SPRY2* is also expressed at high levels surrounding the nasal pits (Szabo-Rogers et al., 2008). At the level of the choanae, there is expression of *Spry2* in the epithelium of the choanae and medial surfaces of the maxillary prominences (Fig. 3.7I'). (Fig. 3.7E). *Spry2* is expressed in the optic nerves as well as in the mandibular epithelium and subadjacent mesenchyme (Fig. 3.7J'). Thus FGF signaling appears to be active in the stomodeal epithelium, especially close the choanae.

Figure 3.7 – *Fgf* pathway genes *Fgfr2* and *Spry2* in *E. subglobosa* stage 3 and 4.

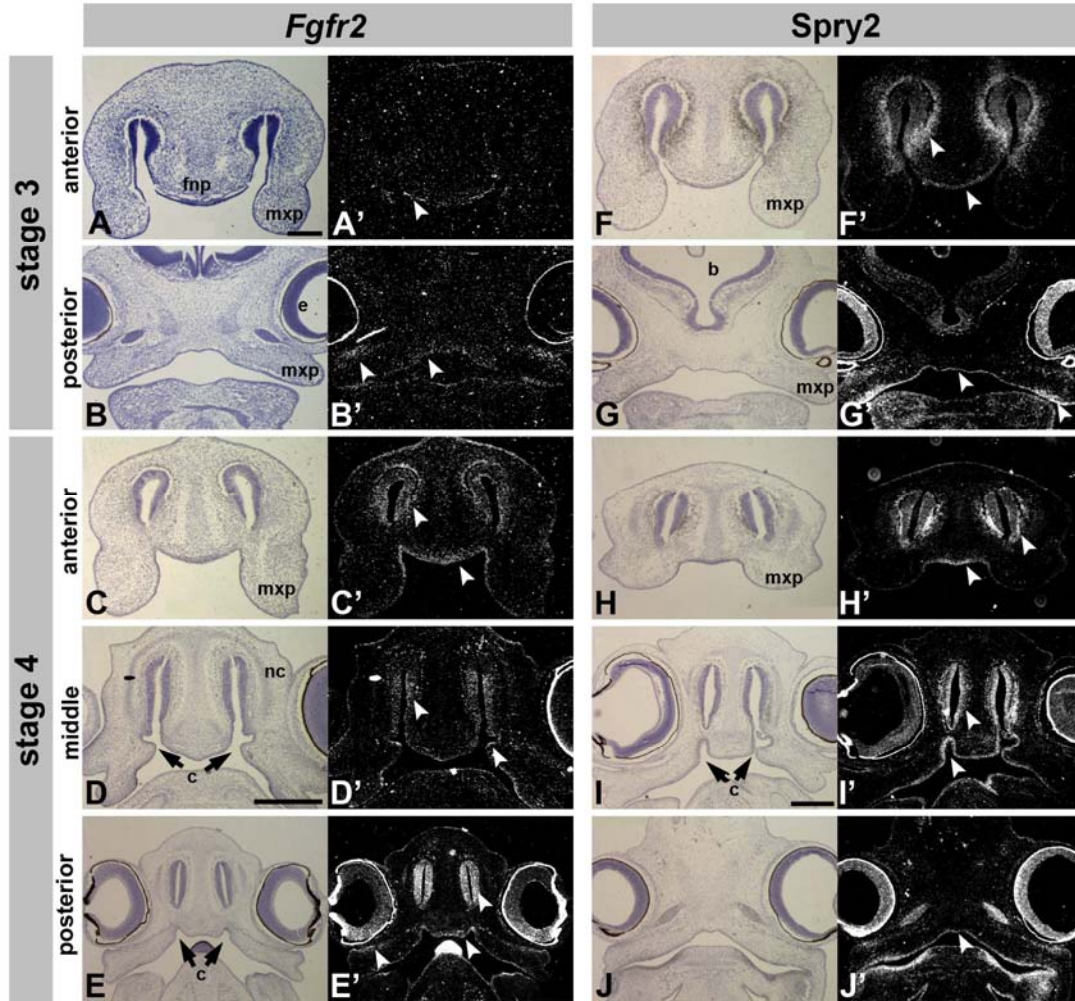


Figure 3.7. Gene expression of *Fgf* pathway genes *Fgfr2*, in stage 3 and 4 embryos. Transverse sections through primary palate (anterior) and presumptive secondary palate (middle and posterior) of *E. subglobosa* at stages 3 and stage 4. *Fgfr2* expression at stage 3 in *E. subglobosa* head is weak, and limited to the oral epithelium of the frontonasal prominence and maxillary prominence (A' and B', arrowheads). By stage 4 strong expression appears across the stomodeal roof (C'). There is also strong expression in the epithelium and mesenchyme surrounding the nasal pits and in the choanae (C', D', E' arrowheads). The strong signal in E' in the middle of the mandible is an artifact. *Spry2* expression surrounding the nasal pits is similar to *Fgfr2* but relatively more abundant. This expression persists across both stages (F', H', I') *Spry2* is also strong in the choanae just before the secondary palate (I' arrowhead) There is also expression in the optic nerve (I', arrowhead). Key: fnp, frontonasal prominence; mxp, maxillary prominence; nc, nasal capsule; c, choanae; Scale bars: A (200 μm) applies to A', B, B', F, F', G, and G'. Scale bar in D (500 μm) applies to D, D', E, E', H, H'. Scale bar in I (500 μm) applies to I, I', J, and J'.

3.3.3 Transcription factors downstream of the Fgf, Hh and BMP signaling pathways are expressed in the turtle palate

Transcription factors known to be downstream of the signaling pathways we had studied was hypothesized to be also expressed during *E. subglobosa* palate development. The genes we investigated were *Msx2* and *Twist1* (Fig. 3.8A-J'). *Msx2* was examined because this homeobox transcription factor is a target of both the Fgf and Bmp pathways (Ashique et al., 2002a; Szabo-Rogers et al., 2008; Higashihori et al., 2010). In addition *Msx2* is required for intramembranous bone formation in mice (Satokata et al., 2000). The basic helix-loop-helix transcription factor *Twist1* is also required for intramembranous bone formation (Bildsoe et al., 2009). FGFs have been shown to positively regulate *Twist* expression in the mouse palate whereas Bmps negatively regulate *Twist1* (O'Rourke and Tam, 2002). In addition *Twist1* can heterodimerize with Gli3 which is a transcription factor in the Hh pathway (O'Rourke and Tam, 2002)

In the primary palate at stage 3, *Msx2* is restricted to the corners of the frontonasal mass and the medial maxillary mesenchyme where fusion will occur (Fig. 3.8A'). *Msx2* expression is also present in the frontonasal and maxillary prominence epithelia (Fig. 3.8A',B'). There is strong expression in midline regions of the mandibular prominence (Fig. 3.8B') similar to the chicken embryo {Mina, 1995 #250}.

In stage 4 embryos, *Msx2* is most strongly expressed in the nasal epithelium (Fig 3.8C'-E'). Anterior sections show elevated mesenchymal expression where frontonasal and lateral nasal prominences have fused, similar to stage 3 and in the caudal frontonasal mass epithelium (Fig 3.8C'). Sections through the choanae and posterior display strong expression in the cleft between the maxillary and mandibular prominences (Fig 3.8D',E').

At stage 3 *Twist1* transcript expression can be seen in the caudal epithelium and mesenchyme of the frontonasal mass and maxillary prominences (Fig. 3.8F',G'). There is also robust expression in mandibular tissue (Fig. 3.8G'). At stage 4 there is abundant mesenchymal *Twist1* signal in the caudal frontonasal mass and maxillary prominences similar to stage 3 (Fig 3.8H'). In deeper sections, through the primitive choanae, there is strong expression around the opening to the nasal passages (Fig. 3.8I'). Posterior to the

choanae, there is robust expression in stomodeal mesenchyme closest to the oral cavity adjacent to the presumptive palatine bone condensations (Fig 3.8J').

Thus several genes are expressed in the stomodeal epithelium and mesenchyme including *Bmp7*, *Ptch1*, *Fgfr2*, *Twist1*. These may indicate that the roof of the oral cavity has retained a stomodeal expression pattern which is distinct from that of the oral surface of the palatal shelves in mammals. In addition the medial edges of the maxillary prominences express *Msx2*, *Twist1*, *Bmp4* and *Ptch1* all of which are also expressed on the medial side of chicken maxillary prominences (Francis-West et al., 1994; Barlow and Francis-West, 1997; Hu and Helms, 1999; Tavares et al., 2001; Ashique et al., 2002a; Higashihori et al., 2010). However there are some differences such as the absence of *Spry2* expression in the turtle maxillary prominences and absence of *Fgfr2* in cartilages both of which are the opposite in chicken embryos (Wilke et al., 1997; Szabo-Rogers et al., 2008). Thus for the most part the chicken and turtle have similar gene expression patterns in the face.

Figure 3.8 - Msx2 and Twist1 Gene Expression in *E. subglobosa* stage 3 and 4

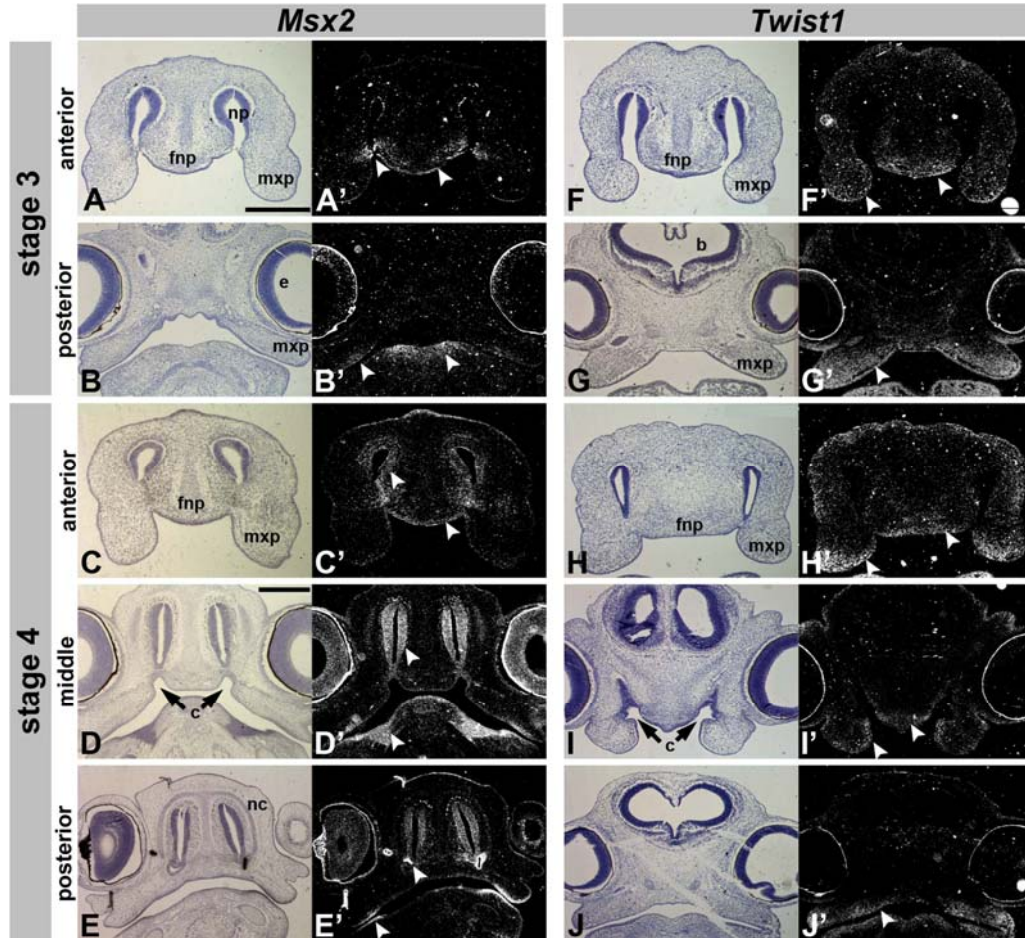


Figure 3.8. Gene Expression of Msx2 and Twist1 transcription factors in *E. subglobosa* stage 3 and 4. Transverse sections through primary palate (anterior) and presumptive secondary palate (middle and posterior) of *E. subglobosa* at stages 3 (A, A', B, B', F, F', G, G') and stage 4 (C, C', D, D', E, E', H, H', I, I', J, J'). Msx2 expression at stage 3 is localized to regions of primary fusion between the frontonasal prominence and the maxillary prominences (A' arrowhead). This pattern persists at stage 4 even after fusion of primary palate (C'). Mandibular mesenchyme shows strong midline expression (B' and D'). Expression of Msx2 is not observed in the choanae (D'). Twist1 is mesenchymally expressed in a relatively wide area of tissue at both stage 3 and 4. Mesenchymal regions closest to the oral cavity express Twist1 at these stages, along with corresponding oral epithelium. Key: fnp, frontonasal prominence, np, nasal passage, mxp, maxillary prominence; e, eye; c, choanae; nc, nasal capsule; b, brain. Scale bar: 500 μ m.

3.4 *Molecular phylogeny of Emydura subglobosa genes*

The *in situ* hybridization experiments on *E. subglobosa* were supportive of a close link to avian amniotes by virtue of the similarity of expression patterns. However we wanted to explore this further using protein sequence alignments. In addition we wanted to confirm that the identity of the clones was correct and that we had indeed isolated the relevant orthologues. Unfortunately, the only reference genome sequence that exists for a non-avian reptile is for *Anolis carolinensis*. This sequence has only been partly annotated and available for searching on the Ensemble database. DNA clones for select turtle sequences have been deposited in Genbank databases, however none exist for our species, *E. subglobosa*. The species of turtle that have mainly been investigated at the molecular level so far are *Pelodiscus sinensis* mainly from Japanese groups and *Trachemys scripta* which has been studied by J. Moustakas, S. Gilbert and several other authors. Other individual clones for snake and gecko were cloned in the Richman lab and are published on Genbank. In contrast, full genome sequence is published for mouse, human and chicken. In conclusion, by comparison to mammals much less is known about reptilian genomes.

Figure 3.9 – Bmp, Fgfr2, and Ptch1 protein phylogeny and orthology

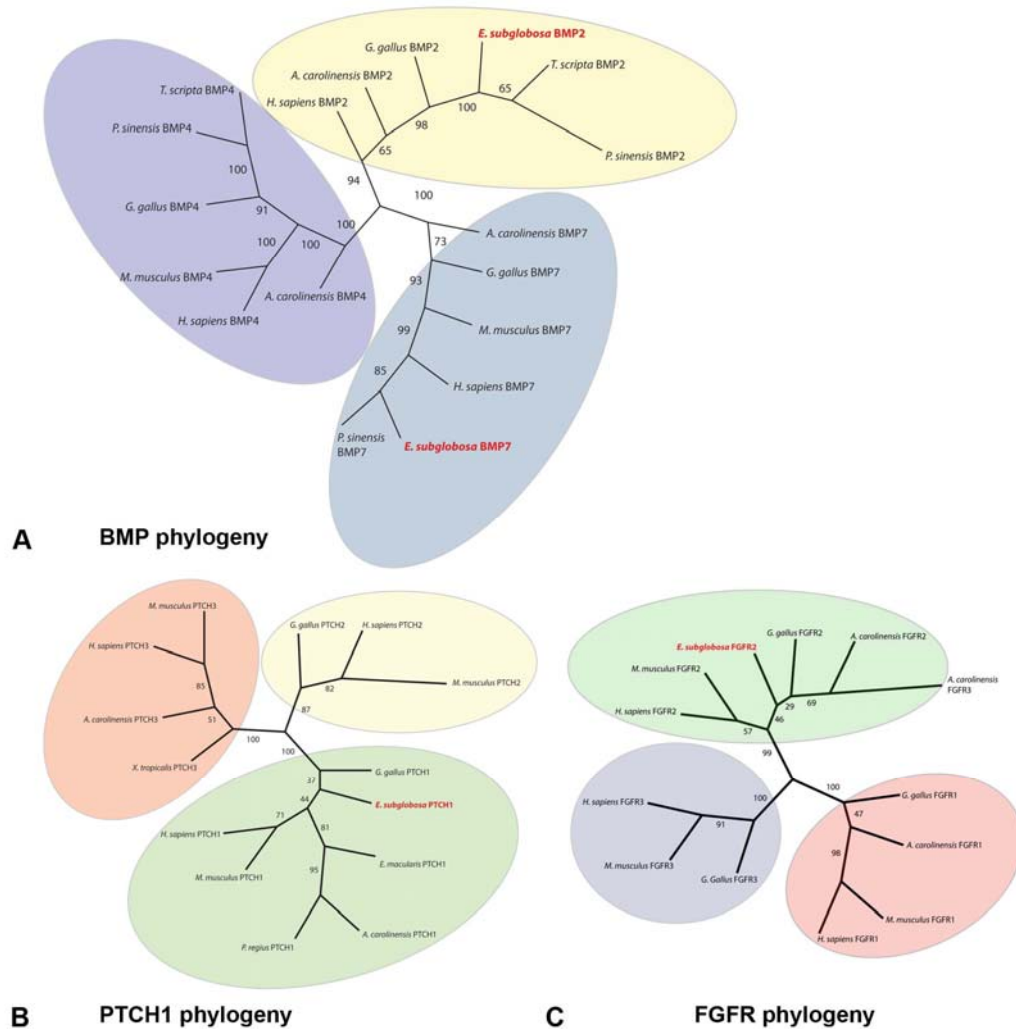


Figure 3.9. Bmp, Fgfr2, and Ptch1 protein phylogeny and orthology. Unrooted phylogenetic trees were created by PHYLIP suite and calculated by neighbour-joining methods. Numerical values denote bootstrap values after 100 tests, and turtle gene of interested is boxed in red. *E. subglobosa* Bmp2 and Bmp7 nested strongly into their respective ligand subgroups and were both similar to other turtle sequences of *T. scripta* and *P. sinensis* (A). *E. subglobosa* Fgfr2 was interestingly predicted as closest to the chicken sequence, and distant to its reptilian cousin *A. carolinensis*. (B). *E. subglobosa* Ptch1, similar to Fgfr2, grouped most closely to the chicken (*G. gallus*) while reptilian cousins the gecko (*E. macularis*), lizard (*A. carolinensis*) and snake (*P. regius*) separated into their own clade.

Table 3.2. Accession numbers of phylogenetic tree sequences

Protein of Interest	Species and Accession Number
BMP2	<i>A. carolinensis</i> : XP_003215357.1; <i>G. gallus</i> : NP_989689.1; <i>H. sapiens</i> : ACV32591.1; <i>P. sinensis</i> : BAD23949.1; <i>T. scripta</i> : AAR03824.2;
BMP4	<i>A. carolinensis</i> : XP_003229120.1; <i>G. Gallus</i> : NP_990568.2; <i>H. Sapiens</i> : NP_001193.2; <i>M. musculus</i> : NP_031580.2; <i>P. sinensis</i> : BAD23950.1
BMP7	<i>A. carolinensis</i> : XP_003223787.1; <i>G. gallus</i> : AAF34179.1; <i>H. sapiens</i> : CAM28318.1; <i>M. musculus</i> : NP_034336.2
FGFR1	<i>A. carolinensis</i> : XP_003226889.1; <i>G. gallus</i> : NP_990841.1; <i>H. sapiens</i> : NP_075598.2; <i>M. musculus</i> : NP_034336.2
FGFR2	<i>A. carolinensis</i> : XP_003218657.1; <i>G. gallus</i> : NP_990650.1; <i>H. sapiens</i> : NP_001138391.1; <i>M. musculus</i> : AAI51202.1
FGFR3	<i>A. carolinensis</i> : XP_03218657.1; <i>G. gallus</i> : NP_990840.2; <i>H. sapiens</i> : NP_000133.1; <i>M. musculus</i> : NP_001192199.1
PTCH1	<i>A. carolinensis</i> : XP_003220312.1; <i>E. macularis</i> : ACY68092.1; <i>G. gallus</i> : NP_990291.1; <i>H. sapiens</i> : NP_001077071.1; <i>M. musculus</i> : NP_032983.1; <i>P. regius</i> : ACY68090.1
PTCH2	<i>G. gallus</i> : AAK97655.1; <i>H. sapiens</i> : AAD17260.1; <i>M. musculus</i> : NP_032984.1
PTCH3	<i>A. carolinensis</i> : XP_003222097.1; <i>H. sapiens</i> : NP_001030014.2; <i>M. musculus</i> : NP_083325.1; <i>X. tropicalis</i> : XP_002933185.1

3.4.1 Bmp phylogenetic analysis

The *in situ* hybridization data suggested that *E. subglobosa* Bmp2, 4 and 7 were expressed in similar patterns to the chicken orthologues (Ashique et al., 2002a; Ashique et al., 2002b; Hu et al., 2008). This led to the hypothesis that the true orthologues for each of these genes was indeed cloned. To test this idea, unrooted phylogenetic trees were created in which orthologues cluster with each other. The *E. subglobosa* cDNAs (513 bp translated sequence of Bmp2 and the 549 bp translated sequence for Bmp7) were included in this analysis. In addition I included Bone Morphogenetic Protein family members from chicken, mouse, human, anolis and other turtle species (Fig. 3.8A).

E. subglobosa Bmp2 and 7 aggregated close to their respective orthologues with strong bootstrap values. In addition turtle sequences clustered together. For example, Bmp2 sequences are available for three turtle species (*E. subglobosa*, *T. scripta*, and *P. sinensis*) and all are close to each other (Fig. 3.8A). A similar close relationship is seen for Bmp7 (*P. sinensis*, *E. subglobosa*) and Bmp4 (*P. sinensis* and *T. scripta*).

Unexpectedly, turtle Bmp7 (*E. subglobosa* and *P. sinensis*) sequences are most similar to human and mouse as opposed to the other reptiles (*G. gallus* and *A. carolinensis*). This relationship may have arisen due to relatively few order-specific mutations being present in Bmp7. Thus it is harder to separate the orthologues in this analysis.

Another unexpected result was the anolis sequences were highly divergent from the turtle sequences. This finding is repeated for each of the Bmps. In contrast, the chicken gene is always positioned close to that of the turtle. This agrees with other molecular phylogeny studies that place turtles close to archosaurs (birds and crocodilians) (Iwabe et al., 2005).

3.4.2 Fgfr phylogenetic analysis:

Unlike the Bmp gene expression patterns, some key differences in *Fgfr2* expression was observed when compared to chicken. The major difference was the lack of expression of *E. subglobosa* in the cartilage. Therefore there was uncertainty as to whether the *E. subglobosa* Fgfr2 clone was the true orthologue of *Fgfr2*. To determine the identity of the clone the same analysis as for the Bmp genes using the translated sequence

derived from the 594 bp clone of *E. subglobosa* *Fgfr2* was carried out. Included were the *Fgfr1*, 2, and 3 proteins in this investigation (Fig. 3.8B).

The different Fgf receptors separated clearly from each other with strong bootstrap values and my *Fgfr2* clone was closely linked to other *Fgfr2* proteins (Fig. 3.8B). This project has established the first ever turtle *Fgfr* clone. However, there was complication in that the *Fgfr3* *A. carolinensis* sequence was nested in the *Fgfr2* branch. The unusual grouping of *Fgfr2* and *Fgfr3* of *A. carolinensis* may be due to the transcript region of *Fgfr2* cloned. This region may be highly conserved and will decrease the probability of sequence divergence between species of animals. With a lack of unique sequence characters, intra-genomic similarities may override orthologous similarities. The unexpected pairing of these two receptors may also stem from the distant evolutionary relationship of *A. carolinensis* to the mammals, aves, and turtle. Once again as for the *Bmps*, *Fgfr2* from *E. subglobosa* is most closely related to the gallus orthologue.

3.4.3 PTCH phylogenetic analysis

The expression patterns of *Ptch1* closely mirrored those of chicken and therefore it was expected that this gene was the true orthologue of *Ptch1* as opposed to closely related genes *Ptch2* and *Ptch3*. The 747 bp translated transcript of *E. subglobosa* as well as sequences from human, mouse, anolis, xenopus, python, and gecko were used in the phylogenetic analysis (Fig. 3.8C). This is the first turtle sequence reported for a *Patched* family member.

The phylogenetic tree displays good separation of the different patched receptors 1-3. The *Ptch1* cloned sequence of *E. subglobosa* branches off from the chicken sequence so once again these two species are closely related. More distant relationships with *A. carolinensis* and *P. regius* *Ptch1* sequences are also revealed. Within *Ptch1* orthologues, mammalian species *H. sapiens* and *M. musculus* branch off together in separate clade. This tree supports the former claim of having cloned *E. subglobosa* *Ptch1*.

CHAPTER 4 - DISCUSSION

4.1 *Palatal shelves are always a precursor to hard palate formation in mammals*

Early constituents of the mammalian head are divided into outgrowths: the frontonasal mass, maxillary prominences, mandibular prominence, and lateral nasal prominences. After soft tissue fusion of the primary palate, palatal shelves start to bud from the medial edges of the maxillary prominences. These palatal shelves are first oriented in vertically, but reorient in the horizontal plane above the tongue as the embryo matures. The palatal shelves extend towards the midline of the head, and the two outgrowths (one from each maxillary prominence) meet at the midline (Gritli-Linde, 2007). Once contact is made, the epithelial cells of the medial edges undergo epithelial-mesenchymal transition (EMT) and ultimately the epithelial seam is lost. This leaves a complete bridge of mesenchyme spanning the oral cavity. It is within the palatal shelf mesenchyme that the palatine bones and palatine processes of the maxillary bones are housed.

In contrast, this project has established that *E. subglobosa* does not form palatal shelves. Therefore the turtle exhibits no midline seam at any point during the corresponding stages studied. Instead, we classify the oral roof as the stomodeal roof and it is continuous across the oral cavity from the first stages of head formation. There is no soft tissue fusion at the secondary palate level of the turtle which is marked by the positions of the future primitive choanae. Instead, the only fusion that takes place is anteriorly in the primary palate. The fusion of the lip or primary palate is completed shortly after stage 3 in *E. subglobosa*.

It is also of interest to note that the mammalian system of palatal shelf formation is also linked to tongue formation. While morphological remodelling of the shelves takes place along the antero-posterior axis in the mouse, the tongue also exhibits coinciding morphological change during this time {Yu, #256}. Other research groups have

postulated that abnormal tongue morphology may attribute to abnormal palatal shelf reorientation from the vertical to horizontal axis. Histological sections of *E. subglobosa* show that while the tongue is present, it is much smaller in relative size to the rest of the head when compared to the mammal. This may be a potential contributor to the lack of shelf formation in the turtle.

4.2 *Posterior choanae tissue may landmark a hotspot for cell signaling in E. subglobosa*

Focal expression of *Bmp2*, *7* and *Ptch1* indicates that Bmp and Hh signaling could be important for induction of the intramembranous palatine bone in our species of turtle. There is evidence from studies in chicken embryos that BMP signaling is able to alter the morphology of the palatine bone. Application of exogenous BMP-2 protein to posterior regions of the maxillary prominences in Hamburger and Hamilton (Hamburger and Hamilton, 1951) stage 20-26 chicks resulted in the abnormal thickening of the palatine bone (Barlow and Francis-West, 1997). Exogenous BMP-2 bead placement into lateral parts of the mandible at H.H. 19/20 also affected the maxillary-derived bones, forming an ectopic palatine bone (Barlow and Francis-West, 1997). There are no studies in chicken in which increasing Shh has affected palatine bone development. However, blocking Hh with cyclopamine inhibits formation of the upper beak including membranous bones (Cordero et al., 2004; Marcucio et al., 2005). Thus of the two signals most highly expressed in the vicinity of the primitive choanae, BMPs seem most likely to be associated with induction of the palatine bones.

Other genes in the tissues anterior and posterior to the choanae were examined and it was found that *Fgfr2* and *Spry2* are also expressed in this region. The evidence from chicken embryos shows that inhibition of *Fgfr2* signaling in the maxillary prominence has no effect on palatal morphogenesis (Szabo-Rogers et al., 2008). In contrast, placing beads in the cranial and lateral side of the frontonasal mass causes cleft lip. Thus the connection between FGFs and palate formation is indirect at this point, secondary to problems with outgrowth of the frontonasal mass.

The two transcription factors that were studied in this project are potential downstream targets of the FGF or BMP signals. However since neither *Msx2* or *Twist1*

are expressed at high levels in the choanae it appears these genes do not play a role in the transduction of BMP or FGF signals in this region. Other genes will need to be studied in future. Elsewhere in the head *Msx2* and *Bmp2,4,7* expression overlap. *Msx2* appears to have a conserved role in primary palate fusion since it has expression on the medial side of the maxillary prominence at stage 3 similar to the chicken {Higashihori, 2010 #120; Szabo-Rogers, 2008 #119}. *Msx2* is also expressed in the midline of the turtle mandibular prominence similar to other amniotes {Mina, 1995 #250}. Both of these regions express *Bmps* in the epithelium. It is possible that *Msx2* mediates Bmp signaling in these other regions. Similarly *Twist1* is strongly expressed in craniofacial mesenchyme and could be acting downstream of Bmps or Fgfs. In the future it is hoped that functional experiments can be designed for the turtle that would allow testing of these hypotheses.

In conclusion, it appears that signaling in the posterior choanae may be helping to specify the cells that are going to form the palatine bone. In addition, signaling in the choanae may be involved in other developmental processes such as formation of the nasal passages. The identification of focused growth factor expression in the choanae is a novel finding not only for turtle but for other amniotes.

4.3 *The mechanism of palate formation of E. subglobosa may be similar to crocodilians*

Palatine bones form a major part of the amniote hard palate. The palatine bones of mammals are posterior bones that make contact anteriorly with the palatine processes of the maxillary bones. In birds, the palatine bones remain separated in the midline, and reach far more anteriorly to touch the premaxillary bone. Consequentially this arrangement of palatine bones creates a naturally cleft oral roof in squamate reptilians and birds. The embryonic development for the reptiles with natural clefts consists of the formation of palatal shelves above the tongue which contain the skeletogenic condensations for the palatine and pterygoid bones

The turtles have a unique morphology that differs from other reptiles since the the anterior hard palate or premaxillary bone is separated from the posterior palate by the choanae which form a communication between the oral and nasal cavities (Gaffney, 1979). Presently it has been shown there is a complete absence of palatal shelves in the

turtle and instead the palatine and pterygoid bones condense directly in the mesenchyme beneath the nasal cavity.

There is third notable variation to palate morphology within the reptilian order: the crocodilians. The palatine bones of the crocodilians are much more similar to mammals and meet in the midline without an opening for the choanae (Ferguson, 1981). Other shared features of the bony palate include the articulation of the palatine bones with palatine processes of the maxillary bone which then make a suture with the premaxillary bone. The only reptilian aspect of the crocodile palate is the presence of the pterygoid bones which form a suture with the palatines. Mammals have vertical pterygoid plates that do not directly contact the palatine bones. The question then arises, do crocodilians have well formed palatal shelves that meet in the midline and fuse? We would hypothesize that mammalian-type palatal shelves are present in crocodilian embryos.

Detailed study of American alligator embryos was carried out by Ferguson (Ferguson, 1979; Ferguson, 1981; Ferguson et al., 1984). In his 1981 paper Ferguson showed frontal sections of crocodilian embryos up to 28 days post oviposition. The sections show rounded palatal swellings forming above the tongue similar to birds and squamate reptiles. The palatal outgrowths were forming at the lateral edges of the oral cavity in the 18 day po embryo (his Fig. 11 and 13). Ferguson then jumped to the 24 day po specimens. In these animals there is continuity of mesenchyme beneath the nasal cavity but does not show the palatal shelves growing together to form a midline seam. He proposes a type of merging is taking place which joins the shelves together. However it is equally possible that the mesenchyme supporting the primitive oral roof proliferates and increases in thickness and that the former palatal swellings become incorporated into this stomodeal mesenchyme. There has been very little molecular work carried out on crocodilians but it would be interesting to see whether their stomodeal roof retains characteristics of the primitive oral cavity rather than oral epithelium of an advanced mammalian-type palate. In the Ferguson study, there are no sections in which specimens have formed intramembranous bones. Thus there persist gaps in knowledge of the crocodilian palate and it may form completely differently than that of mammals. It is therefore still possible that if osseous condensations had been studied, the ontogeny of the

palatal shelves would show them forming beneath the nasal cavity just like in turtles rather than laterally in what previously was the palatal shelf mesenchyme.

4.4 Using palate ontogeny to place turtles in the phylogenetic tree

Interestingly, the pattern of the choanae, palatine and pterygoid bones in *E. subglobosa* is reminiscent of other very primitive extinct turtles, *Proganochelys* (Fig. 1.2). Thus it is likely that at least some extinct turtles also developed in a similar manner to *E. subglobosa*. However, there are other extinct species with a gap in the midline separating the palatine bones and these animals may have been more similar to squamate reptiles and birds during embryogenesis (Gaffney, 1979). Overall turtle palate anatomy supports a basal evolutionary position due to similarities to other basal extinct reptilian amniotes such as captorhinids (Fig. 4.1)(Carroll, 1988) .

The question arises whether the bones of the turtle palate are in fact homologous to mammalian or even other reptilian palatine bones. The adult anatomy supports homology but the ontogeny does not. Presently there are no fate maps existing for turtle neural crest cells but this project has assumed that the neural crest migration in *E. subglobosa* is similar to chickens based on other similarities (sequence homology, gene expression patterns). The stomodeal mesenchyme, in which the turtle palatine bones condense, is most likely, based on avian data, derived from neural crest that migrates ventral to the forebrain and does not originate in any of the facial prominences (Le Lievre, 1978). In contrast, the origins of the avian palatine bones are the proximal and caudal maxillary prominence mesenchyme (Lee et al., 2004) which is derived from mesencephalic and anterior rhombencephalic neural crest cells (Kontges, 1996; Couly et al., 1998). These key differences suggest that turtles generate their palatine bones from a different source of mesenchyme which is consistent with a basal position relative the archosaurs.

It is difficult to determine whether the developmental differences were acquired secondarily (ie. more derived), or whether they represent the most primitive type of palate morphogenesis. In order to investigate this question I examined proliferation and apoptosis patterns carefully. However no evidence supporting rudimentary palatal shelves was obtained. Thus I would conclude these developmental differences could be evidence

for a more basal position of turtles rather than having a shared common ancestor with birds.

4.5 Using molecular phylogeny as a tool for phylogenetic discrimination of turtles

In analyzing Fgfr2, Ptch1, and Bmp2 peptide sequences for *E. subglobosa*, it was surprising to find that the python, gecko, and anole grouped together while the turtle branched most closely with the chicken. Thus the coding sequence data supports *E. subglobosa* as being clustered to the archosaurs (crocodilians and aves). Unfortunately there are very few crocodilian genes cloned and material was available to include homologous genes in the analysis. However it is predicted that since crocodiles are grouped with birds (archosaurs), turtle sequences will be closely related to crocodilian sequences.

Not only did the sequence alignments support a close relationship to *gallus gallus* but so did the patterns of gene expression. The expression of genes in the stomodeum is particularly informative as to which branch the turtles belong. *BMP4*, *BMP7* and *PTCH1* are expressed in the stomodeal epithelium of chickens (Hu et al., 2008) and turtles. However in mouse, the same authors showed that these three genes are not present in the E9.5-10.5 mouse stomodeum (prior to formation of the palatal shelves). Thus gene expression results support *E. subglobosa* as being a reptile and more closely aligned to birds.

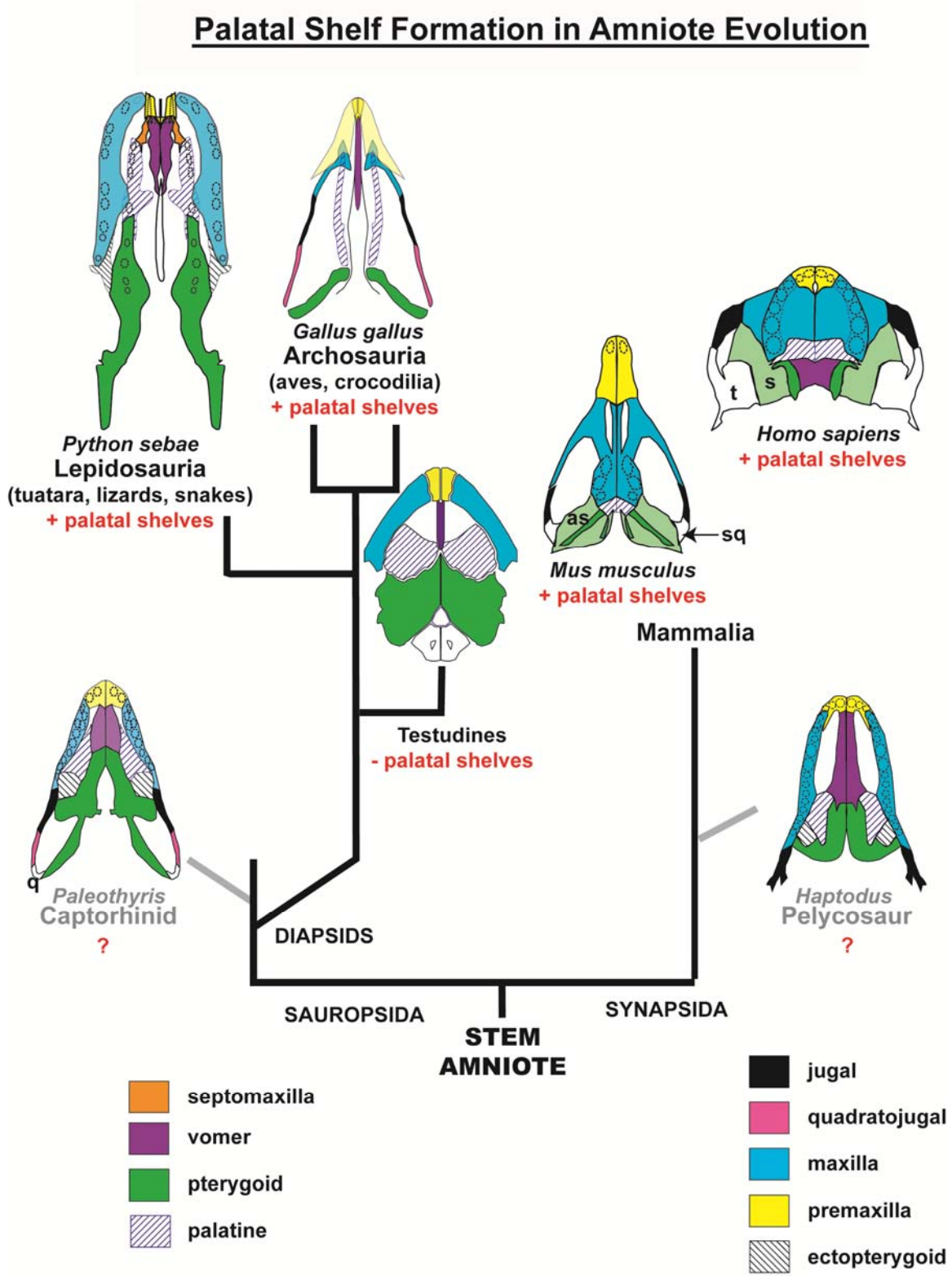
Although gene expression of particular genes seems to support a case for turtles being closely related to the chicken, care must be taken in drawing conclusions. To rule out a more basal position there would need to be a comparison of gene expression patterns to an extinct basal amniote embryo, which clearly is not feasible.

The alternative explanation for why turtles and birds have such a high degree of similarity compared to other reptiles could be the extent of chromosomal rearrangement that took place during evolution. The more rearrangements that took place the higher the sequence divergence and vice versa. Some comparative analysis of chromosomes has been carried out in birds, turtles, crocodilians and mammals. Chromosomal homologies between the chicken and the turtle were found to be highly extensive {Matsuda, 2005 #193}. In addition, comparative mapping of the human, mouse, and chicken displayed 72

predicted chromosome rearrangements between the human and chicken (Burt et al., 1999) . This could indicate that birds had retained an ancestral arrangement of the chromosomes and this is also true for turtles. Once a turtle genome has been sequenced it will be possible to compare the order of genes on chromosomes and examine synteny more carefully.

To fully reconcile all aspects of my data (Table 4.1), a different approach is needed. While the classical transformist seeks to explain evolutionary change as always stemming from ancestral homologs, the emergentist accepts new and novel characters as genuinely unique and not restricted by ancestral origin {Rieppel, 2009 #252;Schmitt, 2005 #253}. When viewing the data from an emergentist point of view, this thesis is able to simply describe the lack of palatal shelf formation as a genuinely unique character that does not require ancestral ties or explanations. This view not only agrees with the data showing a slack of vestigial outgrowth characters, but also allows for all the data to be accounted for without pigeonholing the results as a complex story of morphological transformation.

Figure 4.1. An overview of palatal shelf formation through amniote evolution



4.6 **Conclusions**

This project has characterized the facial ontogeny of *E. subglobosa*. These findings are the first to identify clearly the location of the palatine bones and relate them to the surrounding soft tissues in histological sections. The data taken is from a variety of approaches including anatomical analysis, gene expression, molecular phylogeny and cellular dynamics. Table 4.1 summarizes the arguments for and against a more basal position for turtles. The molecular work puts *E. subglobosa* in a more derived position. However, one may also argue that the complete absence of vestigial palatal shelves in cellular dynamics studies could be used to support a more basal position. Similarly the anatomy of the hard palate places the turtle more basal. Thus we have equal support for both basal and derived placement of *E. subglobosa* in the evolutionary tree. In the future, studies on different aspects of development of the turtle such as formation of the flat, post-orbital skull may assist in concluding a more definitive position for turtles in the evolution of amniotes. Finally, it is anticipated that this work will encourage others to study ontogeny of other turtle species and other reptiles since this is a powerful yet underused tool.

Table 4.1. Arguments for the evolutionary placement of the turtle derived from data in this thesis

Basal Placement	Derived Placement
<ol style="list-style-type: none"> 1. Primitive anatomy eg. large primary choanae, contribution of vomer and pterygoid to the hard palate, palatine bone articulating with pterygoid. 2. Lack of palatal shelf formation throughout secondary palate. No evidence of vestigial shelves: <ol style="list-style-type: none"> a. No increase in cell death in medial maxillary prominences b. No decrease in cell proliferation in maxillary 3. Oral roof identity is primitive: <ol style="list-style-type: none"> a. Retains stomodeal gene expression so the roof of the oral cavity is in fact the stomodeum or undersurface of the nasal cavity. 4. Palatine bones in <i>E. subglobosa</i> are derived from more anterior neural crest than birds or mammals. 	<ol style="list-style-type: none"> 1. Protein sequence homology of signaling ligands and receptors most similar to <i>G. gallus</i> and less similar to squamates. Since birds are considered the most recent radiation of reptiles, these data argue for a derived position. 2. Gene expression similar to chicken <ul style="list-style-type: none"> • Primitive roof exhibits gene expression similar to avian stomodeum. • Transcription factors have similar patterns of expression to those in birds

REFERENCES

- Abzhanov A, Protas M, Grant BR, Grant PR, Tabin CJ. 2004. Bmp4 and morphological variation of beaks in Darwin's finches. *Science* 305:1462-1465.
- Abzhanov A, Tzahor E, Lassar AB, Tabin CJ. 2003. Dissimilar regulation of cell differentiation in mesencephalic (cranial) and sacral (trunk) neural crest cells in vitro. *Development* 130:4567-4579.
- Ashique AM, Fu K, Richman JM. 2002a. Endogenous bone morphogenetic proteins regulate outgrowth and epithelial survival during avian lip fusion. *Development* 129:4647-4660.
- Ashique AM, Fu K, Richman JM. 2002b. Signalling via type IA and type IB bone morphogenetic protein receptors (BMPR) regulates intramembranous bone formation, chondrogenesis and feather formation in the chicken embryo. *Int J Dev Biol* 46:243-253.
- Bailey LJ, Minkoff R, Koch WE. 1988. Relative growth rates of maxillary mesenchyme in the chick embryo. *J Craniofac Genet Dev Biol* 8:167-177.
- Barlow AJ, Francis-West PH. 1997. Ectopic application of recombinant BMP-2 and BMP-4 can change patterning of developing chick facial primordia. *Development* 124:391-398.
- Bildsoe H, Loebel DA, Jones VJ, Chen YT, Behringer RR, Tam PP. 2009. Requirement for Twist1 in frontonasal and skull vault development in the mouse embryo. *Dev Biol* 331:176-188.
- Boughner JC, Buchtova M, Fu K, Diewert V, Hallgrimsson B, Richman JM. 2007. Embryonic development of Python sebae - I: Staging criteria and macroscopic skeletal morphogenesis of the head and limbs. *Zoology (Jena)* 110:212-230.
- Buchtova M, Boughner JC, Fu K, Diewert VM, Richman JM. 2007. Embryonic development of Python sebae - II: Craniofacial microscopic anatomy, cell proliferation and apoptosis. *Zoology (Jena)* 110:231-251.
- Burke AC. 2009. Turtles again. *Evol Dev* 11:622-624.
- Burt DW, Bruley C, Dunn IC, Jones CT, Ramage A, Law AS, Morrice DR, Paton IR, Smith J, Windsor D, Sazanov A, Fries R, Waddington D. 1999. The dynamics of chromosome evolution in birds and mammals. *Nature* 402:411-413.
- Cao Y, Sorenson MD, Kumazawa Y, Mindell DP, Hasegawa M. 2000. Phylogenetic position of turtles among amniotes: evidence from mitochondrial and nuclear genes. *Gene* 259:139-148.
- Carroll RL. 1988. *Vertebrate Paleontology and Evolution*. New York: W. H. Freeman and Company.
- Cordero D, Marcucio R, Hu D, Gaffield W, Tapadia M, Helms JA. 2004. Temporal perturbations in sonic hedgehog signaling elicit the spectrum of holoprosencephaly phenotypes. *J Clin Invest* 114:485-494.
- Couly G, Grapin-Botton A, Coltey P, Ruhin B, Le Douarin NM. 1998. Determination of the identity of the derivatives of the cephalic neural crest: incompatibility between Hox gene expression and lower jaw development. *Development* 125:3445-3459.
- Couly GF, Coltey PM, Le Douarin NM. 1993. The triple origin of skull in higher vertebrates: a study in quail-chick chimeras. *Development* 117:409-429.

- Creuzet G, Cañada S. 2005. Patterning the neural crest derivatives during development of the vertebrate head: insights from avian studies. *J Anat* 207:447-459.
- deBraga M, Rieppel O. 1997. Reptile phylogeny and the interrelationships of turtles. *Zoological Journal of the Linnean Society* 120:281-354.
- Ferguson MW. 1979. The american alligator (*Alligator mississippiensis*): a new model for investigating developmental mechanisms in normal and abnormal palate formation. *Med Hypotheses* 5:1079-1090.
- Ferguson MW. 1981. The structure and development of the palate in *Alligator mississippiensis*. *Arch Oral Biol* 26:427-443.
- Ferguson MW, Honig LS, Slavkin HC. 1984. Differentiation of cultured palatal shelves from alligator, chick, and mouse embryos. *Anat Rec* 209:231-249.
- Foppiano S, Hu D, Marcucio RS. 2007. Signaling by bone morphogenetic proteins directs formation of an ectodermal signaling center that regulates craniofacial development. *Dev Biol* 312:103-114.
- Francis-West PH, Tatla T, Brickell PM. 1994. Expression patterns of the bone morphogenetic protein genes *Bmp-4* and *Bmp-2* in the developing chick face suggest a role in outgrowth of the primordia. *Dev Dyn* 201:168-178.
- Gaffney ES. 1975b. A phylogeny and classification of the higher categories of turtles. *Bull Amer Mus Natur Hist* 155:387-436.
- Gaffney ES. 1979. Comparative Cranial Morphology of Recent and Fossil Turtles. *Bulletin of the American Museum of Natural History* 164:69-376.
- Gaffney ES. 1984. Historical analysis of theories of chelonian relationship. *System Zool* 33:282-301.
- Gritli-Linde A. 2007. Molecular control of secondary palate development. *Dev Biol* 301:309-326.
- Hamburger V, Hamilton H. 1951. A series of normal stages in the development of the chick embryo. *J. Morphol.* 88:49-92.
- Handrigan GR, Leung KJ, Richman JM. 2010. Identification of putative dental epithelial stem cells in a lizard with life-long tooth replacement. *Development* 137:3545-3549.
- Handrigan GR, Richman JM. 2010. Autocrine and paracrine Shh signaling are necessary for tooth morphogenesis, but not tooth replacement in snakes and lizards (Squamata). *Dev Biol* 337:171-186.
- Hedges SB, Poling LL. 1999. A molecular phylogeny of reptiles. *Science* 283:998-1001.
- Higashihori N, Buchtova M, Richman JM. 2010. The function and regulation of *TBX22* in avian frontonasal morphogenesis. *Dev Dyn* 239:458-473.
- Hu D, Colnot C, Marcucio RS. 2008. Effect of bone morphogenetic protein signaling on development of the jaw skeleton. *Dev Dyn* 237:3727-3737.
- Hu D, Helms JA. 1999. The role of sonic hedgehog in normal and abnormal craniofacial morphogenesis. *Development* 126:4873-4884.
- Hu D, Marcucio RS. 2009a. A SHH-responsive signaling center in the forebrain regulates craniofacial morphogenesis via the facial ectoderm. *Development* 136:107-116.
- Hu D, Marcucio RS. 2009b. Unique organization of the frontonasal ectodermal zone in birds and mammals. *Dev Biol* 325:200-210.
- Hu D, Marcucio RS, Helms JA. 2003. A zone of frontonasal ectoderm regulates patterning and growth in the face. *Development* 130:1749-1758.

- Iwabe N, Hara Y, Kumazawa Y, Shibamoto K, Saito Y, Miyata T, Katoh K. 2005. Sister group relationship of turtles to the bird-crocodilian clade revealed by nuclear DNA-coded proteins. *Mol Biol Evol* 22:810-813.
- Janes DE, Organ CL, Fujita MK, Shedlock AM, Edwards SV. 2010. Genome Evolution in Reptilia, the Sister Group of Mammals. *Annual Review of Genomics and Human Genetics*, Vol 11 11:239-264.
- Jung T, Lee YM, Kartavtsev Y, Park IS, Kim DS, Lee JS. 2006. The complete mitochondrial genome of the Korean soft-shelled turtle *Pelodiscus sinensis* (Testudines, Trionychidae). *DNA Seq* 17:471-483.
- Kontges ALaG. 1996. Rhombencephalic neural crest segmentation is preserved throughout craniofacial ontogeny. *Development* 122:3229-3242.
- Krenz JG, Naylor GJ, Shaffer HB, Janzen FJ. 2005. Molecular phylogenetics and evolution of turtles. *Mol Phylogenet Evol* 37:178-191.
- Le Douarin N. 1969. Particularites du noyau interphasique chez la caille japonaise (*Coturnix coturnix japonica*), Utilisation de ces particularites comme "marquage biologique" dans des recherches sur les interactions tissulaires et les migrations cellulaires au cours de l'ontogenese. *Bull. Biol. Fr. Belg.* 103:435-542.
- Le Lievre CS. 1978. Participation of neural crest-derived cells in the genesis of the skull in birds. *J Embryol Exp Morphol* 47:17-37.
- Le M, Raxworthy CJ, McCord WP, Mertz L. 2006. A molecular phylogeny of tortoises (Testudines: Testudinidae) based on mitochondrial and nuclear genes. *Mol Phylogenet Evol* 40:517-531.
- Lee SH, Bedard O, Buchtova M, Fu K, Richman JM. 2004. A new origin for the maxillary jaw. *Dev Biol* 276:207-224.
- Lee SH, Fu KK, Hui JN, Richman JM. 2001. Noggin and retinoic acid transform the identity of avian facial prominences. *Nature* 414:909-912.
- Liu W, Sun X, Braut A, Mishina Y, Behringer RR, Mina M, Martin JF. 2005. Distinct functions for Bmp signaling in lip and palate fusion in mice. *Development* 132:1453-1461.
- Lumsden A, Sprawson N, Graham A. 1991. Segmental origin and migration of neural crest cells in the hindbrain region of the chick embryo. *Development* 113:1281-1291.
- Mallarino R, Grant PR, Grant BR, Herrel A, Kuo WP, Abzhanov A. 2011. Two developmental modules establish 3D beak-shape variation in Darwin's finches. *Proc Natl Acad Sci U S A* 108:4057-4062.
- Marcucio RS, Cordero DR, Hu D, Helms JA. 2005. Molecular interactions coordinating the development of the forebrain and face. *Dev Biol* 284:48-61.
- Matsuda Y, Nishida-Umehara C, Tarui H, Kuroiwa A, Yamada K, Isobe T, Ando J, Fujiwara A, Hirao Y, Nishimura O, Ishijima J, Hayashi A, Saito T, Murakami T, Murakami Y, Kuratani S, Agata K. 2005. Highly conserved linkage homology between birds and turtles: Bird and turtle chromosomes are precise counterparts of each other. *Chromosome Research* 13:601-615.
- McGonnell IM, Clarke JD, Tickle C. 1998. Fate map of the developing chick face: analysis of expansion of facial primordia and establishment of the primary palate. *Dev Dyn* 212:102-118.

- Mina M, Gluhak J, Upholt WB, Kollar EJ, Rogers B. 1995. Experimental analysis of Msx-1 and Msx-2 gene expression during chick mandibular morphogenesis. *Dev Dyn* 202:195-214.
- Minkoff R, Kuntz AJ. 1978. Cell proliferation and cell density of mesenchyme in the maxillary process and adjacent regions during facial development in the chick embryo. *J Embryol Exp Morphol* 46:65-74.
- Minowada G, Jarvis LA, Chi CL, Neubuser A, Sun X, Hacohen N, Krasnow MA, Martin GR. 1999. Vertebrate Sprouty genes are induced by FGF signaling and can cause chondrodysplasia when overexpressed. *Development* 126:4465-4475.
- Naro-Maciel E, Le M, FitzSimmons NN, Amato G. 2008. Evolutionary relationships of marine turtles: A molecular phylogeny based on nuclear and mitochondrial genes. *Mol Phylogenet Evol* 49:659-662.
- Noden DM. 1978. The control of avian cephalic neural crest cytodifferentiation. I. Skeletal and connective tissues. *Dev Biol* 67:296-312.
- Noden DM. 1983. The role of the neural crest in patterning of avian cranial skeletal, connective, and muscle tissues. *Dev Biol* 96:144-165.
- O'Rourke MP, Tam PP. 2002. Twist functions in mouse development. *Int J Dev Biol* 46:401-413.
- Ornitz DM, Xu JS, Colvin JS, McEwen DG, MacArthur CA, Coulier F, Gao GX, Goldfarb M. 1996. Receptor specificity of the fibroblast growth factor family. *Journal of Biological Chemistry* 271:15292-15297.
- Parham JF, Macey JR, Papenfuss TJ, Feldman CR, Turkozan O, Polymeni R, Boore J. 2006. The phylogeny of Mediterranean tortoises and their close relatives based on complete mitochondrial genome sequences from museum specimens. *Mol Phylogenet Evol* 38:50-64.
- Pough FH, Janis CM, Heiser JB. 2005. *Vertebrate Life*. Upper Saddle River, New Jersey: Pearson Education Inc., Pearson Prentice Hall. 684 p.
- Rice R, Connor E, Rice DP. 2006. Expression patterns of Hedgehog signalling pathway members during mouse palate development. *Gene Expr Patterns* 6:206-212.
- Richman JM, Buchtova M, Boughner JC. 2006. Comparative ontogeny and phylogeny of the upper jaw skeleton in amniotes. *Dev Dyn* 235:1230-1243.
- Rieppel O. 1999. The origin and early evolution of turtles. *Annual Review of Ecology and Systematics* 30:1-22.
- Rieppel O, deBraga M. 1996. Turtles as diapsid reptiles. *Nature* 384:453-455.
- Rowe A, Richman JM, Brickell PM. 1992. Development of the spatial pattern of retinoic acid receptor-beta transcripts in embryonic chick facial primordia. *Development* 114:805-813.
- Russell RD, Beckenbach AT. 2008. Recoding of translation in turtle mitochondrial genomes: programmed frameshift mutations and evidence of a modified genetic code. *J Mol Evol* 67:682-695.
- Sasaki T, Takahashi K, Nikaido M, Miura S, Yasukawa Y, Okada N. 2004. First application of the SINE (short interspersed repetitive element) method to infer phylogenetic relationships in reptiles: an example from the turtle superfamily Testudinoidea. *Mol Biol Evol* 21:705-715.
- Satokata I, Ma L, Ohshima H, Bei M, Woo I, Nishizawa K, Maeda T, Takano Y, Uchiyama M, Heaney S, Peters H, Tang Z, Maxson R, Maas R. 2000. Msx2

- deficiency in mice causes pleiotropic defects in bone growth and ectodermal organ formation. *Nat Genet* 24:391-395.
- Shaffer HB, Meylan P, McKnight ML. 1997. Tests of turtle phylogeny: molecular, morphological, and paleontological approaches. *Syst Biol* 46:235-268.
- Shah RM, Cheng KM, MacKay RA, Wong A. 1987. Secondary palate development in the domestic duck (Khaki Campbell). An electron microscopic, histochemical, autoradiographic and biochemical study. *J Anat* 154:245-258.
- Shah RM, Crawford BJ. 1980. Development of the secondary palate in chick embryo: a light and electron microscopic and histochemical study. *Invest Cell Pathol* 3:319-328.
- Shah RM, Ogasawara DM, Cheng KM. 1988. Embryogenesis of the secondary palate in pigeons. *Poult Sci* 67:865-870.
- Shedlock AM, Botka CW, Zhao S, Shetty J, Zhang T, Liu JS, Deschavanne PJ, Edwards SV. 2007. Phylogenomics of nonavian reptiles and the structure of the ancestral amniote genome. *Proc Natl Acad Sci U S A* 104:2767-2772.
- Sheil CA. 2003. Osteology and skeletal development of *Apalone spinifera* (Reptilia: Testudines: Trionychidae). *J Morphol* 256:42-78.
- Sheil CA. 2005. Skeletal development of *Macrochelys temminckii* (Reptilia: Testudines: Chelydridae). *J Morphol* 263:71-106.
- Spinks PQ, Shaffer HB. 2009. Conflicting mitochondrial and nuclear phylogenies for the widely disjunct *Emys* (Testudines: Emydidae) species complex, and what they tell us about biogeography and hybridization. *Syst Biol* 58:1-20.
- Spinks PQ, Thomson RC, Lovely GA, Shaffer HB. 2009. Assessing what is needed to resolve a molecular phylogeny: simulations and empirical data from emydid turtles. *BMC Evol Biol* 9:56.
- Szabo-Rogers HL, Geetha-Loganathan P, Nimmagadda S, Fu KK, Richman JM. 2008. FGF signals from the nasal pit are necessary for normal facial morphogenesis. *Dev Biol* 318:289-302.
- Tavares AT, Izpisua-Belmonte JC, Rodriguez-Leon J. 2001. Developmental expression of chick twist and its regulation during limb patterning. *Int J Dev Biol* 45:707-713.
- Tulenko FJ, Sheil CA. 2007. Formation of the chondrocranium of *Trachemys scripta* (Reptilia: Testudines: Emydidae) and a comparison with other described turtle taxa. *J Morphol* 268:127-151.
- Valenzuela N. 2009. The painted turtle, *Chrysemys picta*: a model system for vertebrate evolution, ecology, and human health. *Cold Spring Harb Protoc* 2009:pdb emo124.
- Werneburg I, Hugi J, Muller J, Sanchez-Villagra MR. 2009. Embryogenesis and ossification of *Emydura subglobosa* (Testudines, Pleurodira, Chelidae) and patterns of turtle development. *Dev Dyn* 238:2770-2786.
- Werneburg I, Sanchez-Villagra MR. 2009. Timing of organogenesis support basal position of turtles in the amniote tree of life. *Bmc Evolutionary Biology* 9:-.
- Wilke TA, Gubbels S, Schwartz J, Richman JM. 1997. Expression of fibroblast growth factor receptors (FGFR1, FGFR2, FGFR3) in the developing head and face. *Dev Dyn* 210:41-52.

- Wu P, Jiang TX, Shen JY, Widelitz RB, Chuong CM. 2006. Morphoregulation of avian beaks: comparative mapping of growth zone activities and morphological evolution. *Dev Dyn* 235:1400-1412.
- Wu P, Jiang TX, Suksaweang S, Widelitz RB, Chuong CM. 2004. Molecular shaping of the beak. *Science* 305:1465-1466.
- Zardoya R, Meyer A. 1998. Complete mitochondrial genome suggests diapsid affinities of turtles. *Proc Natl Acad Sci U S A* 95:14226-14231.
- Zardoya R, Meyer A. 2001. The evolutionary position of turtles revised. *Naturwissenschaften* 88:193-200.
- Zhang L, Nie L, Cao C, Zhan Y. 2008. The complete mitochondrial genome of the Keeled box turtle *Pyxidea mouhotii* and phylogenetic analysis of major turtle groups. *J Genet Genomics* 35:33-40.
- Zhou Z. 2004. The origin and early evolution of birds: discoveries, disputes, and perspectives from fossil evidence. *Naturwissenschaften* 91:455-471.